

Technical appendix

Methods used by WHO to estimate the global burden of TB disease for publication in the global tuberculosis report 2024

29 October 2024

Contents

| | |
|--|----|
| Abstract | 4 |
| 1. Introduction | 6 |
| 2. Historical background | 7 |
| 3. Incidence of TB, 2000–2019..... | 8 |
| 3.1 Five main methods to estimate TB incidence | 10 |
| 3.1.1 Method 1 - Results from TB prevalence surveys | 10 |
| 3.1.2 Method 2 – Results from a national TB prevalence survey combined with a country-specific dynamic model..... | 11 |
| 3.1.3 Method 3 - Case notification data combined with expert opinion about case detection gaps..... | 13 |
| 3.1.4 Method 4 - Notifications in high-income countries adjusted by a standard factor to account for under-reporting and under-diagnosis | 15 |
| 3.1.5 Method 5 - Inventory studies, capture-recapture modelling..... | 15 |
| 3.2 TB incidence in people living with HIV | 17 |
| 4. Mortality caused by TB, 2000–2019 | 19 |
| 4.1 Estimating TB mortality among HIV-negative people from vital registration data and mortality surveys up to 2019 | 19 |
| 4.2 Estimates of the number of deaths caused by TB in India | 20 |
| 4.3 Estimating TB mortality among HIV-negative people from estimates of case fatality rates and TB incidence | 22 |
| 4.4 Estimating TB mortality among people living with HIV | 23 |
| 5. Estimation of uncertainty, 2000–2019 | 25 |
| 6. Estimation of the impact of COVID-19 on the burden of TB, 2020–2023 | 26 |
| 6.1 Country-specific dynamic models..... | 26 |
| 6.1.1 Model overview | 27 |
| 6.1.2 Model equations | 28 |
| 6.1.3 Implementation | 30 |
| 6.1.4 Data and calibration..... | 32 |
| 6.1.5 Modelling disruptions to TB services..... | 33 |
| 6.1.6 Model limitations..... | 35 |
| 6.2 Region-specific dynamic models..... | 40 |
| 7. Disaggregation of TB incidence and mortality by age and sex, 2023 | 42 |
| 7.1 TB incidence | 42 |

| | |
|--|----|
| 7.2 TB mortality..... | 44 |
| 8. Drug-resistant TB - incidence and proportions with resistance | 45 |
| 8.1 Proportions of new and previously treated TB cases with rifampicin resistance | 45 |
| 8.2 Incidence of RR-TB | 46 |
| 8.3 Proportion of RR-TB cases with resistance to fluoroquinolones (pre-XDR-TB)..... | 47 |
| 9. Drug-resistant TB - mortality | 48 |
| 10. Deaths averted by TB interventions | 49 |
| 11. Household contacts of bacteriologically confirmed pulmonary TB eligible for TB preventive therapy (TPT)..... | 50 |
| 12. Excess number of deaths caused by TB during the COVID-19 pandemic and its aftermath, 2020–2023 | 52 |
| 13. Attributable risk for TB..... | 53 |
| 13.1 Risk ratios..... | 53 |
| 13.2 Exposed population | 54 |
| 13.3 Population attributable fraction | 55 |
| 13.4 Attributable TB cases | 55 |
| 14. Conclusion..... | 57 |
| Acknowledgements..... | 58 |
| Annex 1 - Definitions..... | 59 |
| References | 60 |

Abstract

This technical appendix describes methods used by WHO in 2024 to estimate the following: tuberculosis (TB) incidence and mortality for the period 2010–2023; TB incidence and mortality disaggregated by age and sex for 2023; proportion of TB cases with rifampicin-resistant (RR) TB, which includes multidrug-resistant (MDR) TB (together referred to as MDR/RR-TB), and incidence of MDR/RR-TB for the period of 2015–2023; mortality due to MDR/RR-TB in 2023; proportion of MDR/RR-TB cases with fluoroquinolone resistance (pre-extensively drug-resistant TB, pre-XDR-TB) in 2023; number of deaths averted by TB interventions from 2010–2023; number of household contacts of bacteriologically confirmed pulmonary TB cases aged under 5 years and eligible for TB preventive therapy (TPT) in 2015–2023; and attributable risk for TB in 2023.

Four main methods are used to derive incidence over the period 2010–2019: (i) results from TB prevalence surveys; (ii) notifications in high-income countries adjusted by a standard factor to account for under-reporting and underdiagnosis and (iii) national inventory studies; (iv) case notification data combined with expert opinion about case detection gaps. Mortality is obtained from national vital registration systems of mortality surveys, where available. In other countries, mortality is derived indirectly from estimates for incidence and case fatality ratio.

For the years 2020 to 2023, TB incidence and mortality are estimated using dynamic models for 24 countries. Such models were used for countries with large absolute reductions in the reported number of people newly diagnosed with TB in 2020 or 2021 (case notifications) relative to pre-2020 trends; these reductions were interpreted as being due to reduced detection of people with TB. Although individual countries may have reported large relative reductions in case notifications, in absolute terms these reductions may not have been sufficient to warrant their inclusion in the country-specific modelling described above. Instead, region-specific models were used for 23 countries that reported a cumulative reduction in TB case notifications of 10% or more in 2020 to 2021 inclusive, relative to pre-2020 trends.

Estimates of TB incidence and mortality in all high-income countries in 2020–2023 were produced using the same methods as those used in 2010–2019; that is, notification data with a standard adjustment for incidence, and vital registration (VR) data for mortality. For low- and middle-

income countries (LMIC) that were not modelled (i.e. those for which case notifications in 2020 and 2021 did not show a substantial reduction relative to pre-2020 trends), the methods used to estimate TB incidence and mortality before 2020 were retained for use in 2020–2023, with the assumption that pre-2020 trends continued in 2020–2023.

The new methods developed in 2022 to allow the production of time series of estimates of the incidence of MDR/RR-TB were retained for the period 2015–2023. The time series are for the absolute number of incident MDR/RR-TB cases and the proportions of TB cases (new and previously treated) that have MDR/RR-TB.

Code for implementing the described methods is available in a public [repository](#).

1. Introduction

Estimates of the burden of disease caused by TB and measured in terms of incidence and mortality are produced annually by WHO using information gathered through surveillance systems (case notifications and death registrations), special studies (including surveys of the prevalence of disease), mortality surveys, “inventory studies” of under-reporting of detected TB, in-depth analysis of surveillance and other data, expert opinion and consultations with countries. In June 2006, the WHO Task Force on TB Impact Measurement was established,[1] to ensure robust, rigorous and consensus-based assessment of progress towards milestones and targets for reductions in TB disease. The Task Force reviewed methods and provided recommendations in 2008, 2009, 2015, 2016, 2019 and 2022. The most recent meeting of the Task Force was held in September 2024 to review and propose new options for estimating TB incidence and mortality. Updates based on the outcomes of this meeting are expected to be incorporated in future Global TB Reports.

Code for implementing the described methods is available in a public [repository](#).

2. Historical background

Historically, a major source of data to derive incidence estimates were results from tuberculin surveys conducted in children [2]. Early studies showed the following relationship between the annual risk of infection denoted λ and the incidence of smear positive TB denoted I_{s+} : one smear positive case infects on average 10 individuals per year for a period of 2 years and a risk of infection of $10^{-2}y^{-1}$ corresponds approximately to an incidence rate of $50 \times 10^{-5}y^{-1}$. However, this relationship no longer holds in the context of modern TB control and in settings with a high prevalence of HIV [3]. In addition to uncertainty about the relationship between λ and I_{s+} , estimates of incidence obtained from tuberculin surveys suffer from other sources of uncertainty and bias, including unpredictable diagnostic performance of the tuberculin test [4], digit preference when reading and recording the size of tuberculin reactions,[5] sensitivity to assumptions about reaction sizes attributed to infection[6], sensitivity to the common assumption that the annual risk of infection is age invariant, and lastly, sensitivity of overall TB incidence estimates to the assumed proportion of TB incidence that is smear positive.

A first global and systematic estimation exercise led by WHO in the early 1990s estimated that there were approximately 8 million incident TB cases in 1990 ($152 \times 10^{-5}y^{-1}$) and 2.6-2.9 million deaths ($46 - 55 \times 10^{-5}y^{-1}$) [7]. A second major reassessment was published in 1999 [8], with an estimated 8 million incident cases for the year 1997 ($136 \times 10^{-5}y^{-1}$), and 1.9 million TB deaths ($32 \times 10^{-5}y^{-1}$). The most important sources of information were case notification data for which gaps in detection and reporting were obtained from expert opinion. In addition, data from 24 tuberculin surveys were translated into incidence and 29 national TB prevalence surveys were used.

3. Incidence of TB, 2000–2019

TB incidence has never been measured through population–based surveys at the national level because this would require long-term studies among large cohorts of people (hundreds of thousands of people), involving high costs and challenging logistics. Notifications of TB cases provide a good proxy indication of TB incidence in countries that have both high-performance surveillance systems (where there is little under-reporting of diagnosed cases) and where the quality of and access to health care means that few cases remain undiagnosed and overdiagnosis is limited. In the large number of countries where these criteria are not yet met, better estimates of TB incidence can be obtained from an inventory study. An inventory study aims at quantifying the level of under-reporting of detected TB cases; if certain conditions are met, capture-recapture methods can also be used to estimate TB incidence [9].

The goal of TB surveillance is to directly measure TB incidence from national case notifications in all countries. This requires a combination of strengthened surveillance, better quantification of under-reporting and over-reporting (i.e. the number of newly diagnosed cases that are missed by surveillance systems and the number of cases over-diagnosed with TB) and universal access to quality health care (to minimize under-diagnosis of cases and overdiagnosis). A TB surveillance checklist developed by the WHO Global Task Force on TB Impact Measurement defines the standards that need to be met for notification data to provide a direct measure of TB incidence [10].

Methods used for the period 2000–2019 by WHO to estimate TB incidence can be grouped into four major categories. The distribution of countries according to the four categories are shown in [Figure 1.1.12](#) of the web content of WHO's *Global tuberculosis report 2024* - in practice, methods are often combined to estimate the entire time series and the distribution of countries shown reflects the main method used to estimate incidence over the most recent years up to 2019.

1. **Results from TB prevalence surveys.** This method is used for 28 countries, that accounted for 39% of the estimated global number of incident cases in 2019.

2. **Results from a national TB prevalence survey combined with a country-specific dynamic model.** This method is used for India, which accounted for 27% of the global number of incident TB cases in 2019.
3. **Case notification data combined with expert opinion about case detection gaps.** This method is used for 39 countries that accounted for 11% of the estimated global number of incident cases in 2019.
4. **Notifications in high-income countries adjusted by a standard factor to account for under-reporting, under-diagnosis and overdiagnosis/overreporting.** This method was used for 137 countries that comprise all high-income countries except France, Germany, the Netherlands, the Republic of Korea and the United Kingdom, plus selected upper-middle income countries with low levels of underreporting, including Brazil, China and the Russian Federation. These 137 countries accounted for 6% of the estimated global number of incident cases in 2019.
5. **Results from inventory/capture-recapture studies.** This method is used for 10 countries: China, Egypt, France, Germany, Indonesia, Iraq, the Netherlands, the Republic of Korea, the United Kingdom and Yemen. They accounted for 17% of the estimated global number of incident cases in 2019.

3.1 Five main methods to estimate TB incidence

3.1.1 Method 1 - Results from TB prevalence surveys

TB incidence is estimated using measurements from national surveys of the prevalence of TB disease combined with estimates of the duration of disease. Incidence is estimated as the prevalence of TB divided by the average duration of disease assuming epidemic equilibrium: let N denote the size of a closed population with the number of birth and deaths the same for a period $\Delta t > 0$, let C be the number of prevalent TB cases, P the prevalence rate so that $P = C/N$. Let m denote the rate of exit from the pool of prevalent cases through mortality, spontaneous self-cure or cure from treatment, and I the rate at which new cases are added to the pool. At equilibrium during the time period Δt and further assuming exponentially distributed durations d such that $d = m^{-1}$

$$I(N - C) = mC$$

$$I = \frac{mC}{N - C} = \frac{P}{d(1 - P)} \approx \frac{P}{d}$$

In practice, the average duration of presence in the pool of prevalent cases cannot be directly measured. For example, measurements of the duration of symptoms in prevalent TB cases that are detected during a prevalence survey are systematically biased towards lower values, since survey investigations truncate the natural history of undiagnosed disease. Measurements of the duration of disease in notified cases ignore the duration of disease among non-notified cases and are affected by recall biases.

Literature reviews have provided estimates of duration of disease in untreated TB cases from the pre-chemotherapy era (before the 1950s). The best estimate of the mean duration of untreated disease (for smear-positive and smear-negative cases combined) in HIV-negative individuals is about three years. There are few data available on the duration of disease in people living with HIV. The assumed distributions of disease durations are shown in Table 1. An alternative approach is to estimate the duration of disease indirectly, using data from prevalence surveys on the proportion of prevalent TB that were on TB treatment.

Table 1. Distribution of disease duration by case category

| Case category | Distribution of disease duration (year) |
|-------------------------------------|---|
| Treated, HIV-negative | Uniform (0.2–2) |
| Not treated, HIV-negative | Uniform (1–4) |
| Treated, people living with HIV | Uniform (0.01–1) |
| Not treated, people living with HIV | Uniform (0.01–0.2) |

3.1.2 Method 2 – Results from a national TB prevalence survey combined with a country-specific dynamic model.

In previous years, TB burden estimates in India were informed partly by results from a state-level prevalence survey from Gujarat. However, India has recently completed a national prevalence survey, which offers the opportunity to update earlier estimates with nationally representative data. In addition, new data such as drug sales in the private healthcare sector have also been available to inform burden estimates. To incorporate these different sources of evidence, a country-specific model was developed in 2022 to produce “interim” estimates of TB incidence for the period 2010–2019. This model has been extensively reviewed in 2023, also incorporating additional data for TB burden, to produce an updated time series of TB incidence for the period 2010–2019.

The main data incorporated into the model are:

- National TB prevalence survey data (2020)
- National TB case notifications in 2011 and 2019
- Pre-pandemic mortality estimates, 2015 and 2019, WHO (informed by the Sample Registration System, a source for vital registration data in India)

- Volumes of anti-TB drugs sold by the private healthcare sector from 2015-2019, to inform trends in the numbers of patients managed by the private sector managed by private sector
- Estimates for the prevalence of TB infection drawn from a TB infection survey that accompanied the recent prevalence survey in 2019
- COVID-19 Community mobility reports from Google, to inform assumptions about periods during which TB transmission was reduced.

The structure of the model is shown in Figure 1.

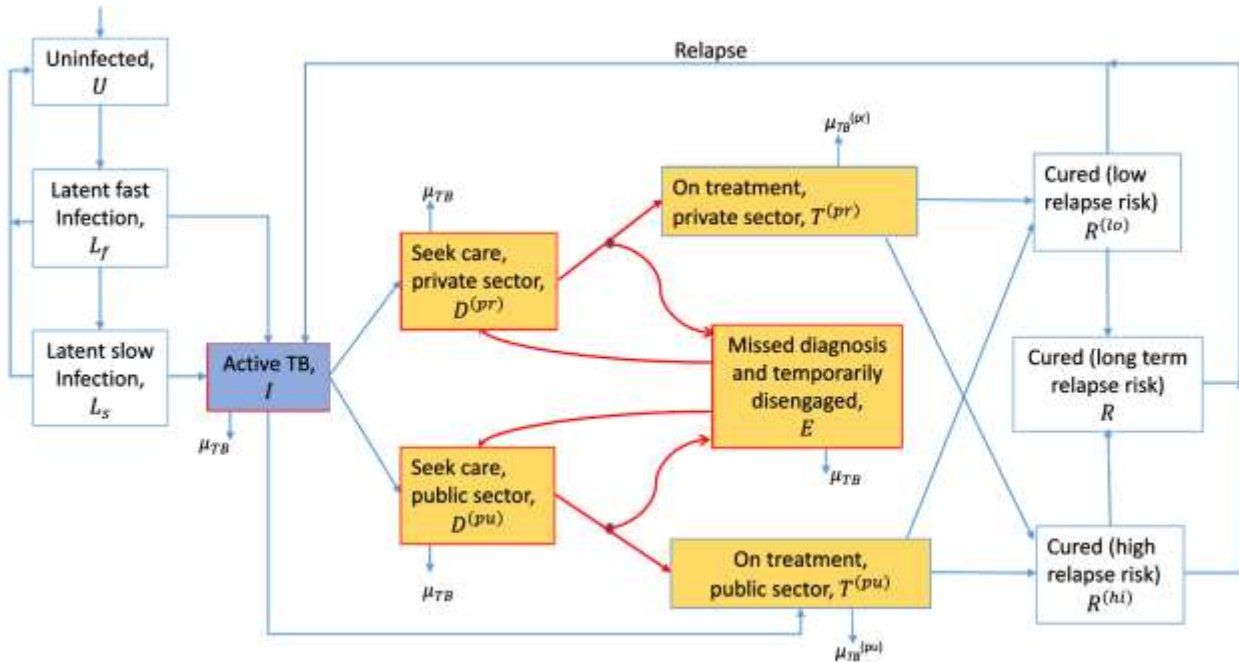


Figure 1. Schematic illustration of the model structure used for burden estimation in India. All colored boxes correspond to model states whose sizes were informed by India's prevalence survey. The box in blue corresponds to the proportion of prevalent TB that had not sought care (including subclinical and symptomatic TB), while the boxes in yellow correspond to the proportion of prevalent TB that had sought care. This model is similar to that used for other countries, with the key differences being: (i) the inclusion of compartments for those awaiting diagnosis (labelled 'Seek care'), and (ii) The data used to calibrate the model (see text).

Full model equations are given in a publication on this model¹, with the caveat that the current version of the model (used in the *Global tuberculosis report 2024*) was calibrated to updated estimates of TB mortality, that are nonetheless comparable to those used in the publication.

3.1.3 Method 3 - Case notification data combined with expert opinion about case detection gaps

Expert opinion, elicited in regional workshops, national consensus workshops or country missions, is used to estimate levels of under-reporting, over-reporting (false positive diagnoses that may occur particularly in the context of systematic screening in populations with relatively low probability of TB disease) and under-diagnosis. Trends are estimated using either mortality data, national repeat surveys of the annual risk of infection or exponential interpolation using estimates of case detection gaps for specific years. The estimation of case detection gaps is essentially based on an in-depth analysis of surveillance data; experts provide their educated best guess about the range of the plausible detection gap g and incidence I is obtained from

$$I = \frac{f(N)}{1 - g}, g \in [0,1]$$

where N denotes case notifications, and f denotes a cubic spline function in countries with large year-to-year fluctuations in N , or else, the identity function. The incidence series are completed using assumptions about changes in case fatality rate (CFR) over time in countries with evidence of improvements in TB prevention and care, such as increased detection coverage over time or improved treatment outcomes, ensuring that the following inequality holds

$$0 \leq \left| \frac{\Delta I}{\Delta t} \right| \leq \left| \frac{\Delta M}{\Delta t} \right|$$

where M denotes mortality.

A full description of the methods used in regional workshops where expert opinion was systematically elicited following an in-depth analysis of surveillance data is publicly available in a

¹ Mandal S, Rao R, Joshi R. Estimating the Burden of Tuberculosis in India: A Modelling Study. Indian J Community Med. 2023 May-Jun;48(3):436-442. doi: 10.4103/ijcm.ijcm_160_23. Epub 2023 Mar 24. PMID: 37469917; PMCID: PMC10353668.

report of the workshop held for countries in the African Region (in Harare, Zimbabwe, December 2010) [11]. In some countries, case reporting coverage changed significantly during the period 2000-2019 as a result of disease surveillance reforms. Trends in incidence are derived from repeat tuberculin survey results in Bhutan and Yemen and from trends in mortality or case notifications.

Case proportions are assumed to follow a beta distribution, with parameters α and β obtained from the expected value E and variance V using the method of moments, as follows

$$\alpha = E \left(\frac{E(1-E)}{V} - 1 \right)$$

$$\beta = (1-E) \left(\frac{E(1-E)}{V} - 1 \right)$$

Time series are built according to the characteristics of the levels of under-reporting and under-diagnosis that were estimated for specific reference years (three reference years in regional workshops conducted around 2010). A cubic spline extrapolation of V and E , with knots set at the reference years, is used for countries with low-level or concentrated HIV epidemics. In countries with a generalized HIV epidemic, the trajectory of incidence is based on the annual rate of change in HIV prevalence and time changes in the fraction F of incidence attributed to HIV, determined as follows

$$F = \frac{h(\rho - 1)}{h(\rho - 1) + 1} = \frac{\theta - h}{1 - h}$$

where h is the prevalence of HIV in the general population, ρ is the TB incidence rate ratio among people living with HIV over HIV-negative individuals and θ is the prevalence of HIV among new TB cases.

If there is insufficient data to determine the factors leading to time-changes in case notifications, incidence is assumed to follow a horizontal trend going through the most recent estimate of incidence.

Limitations of the method based on eliciting expert opinion about gaps in case detection and reporting include a generally small number of interviewed experts; lack of clarity about vested

interests when eliciting expert opinion; lack of recognition of over-reporting (due to over-diagnosis, e.g. in some countries implementing a large-scale systematic population screening policy that may result in many people with abnormal chest X-ray but no bacteriological confirmation of TB disease being notified and treated as new TB cases) or in countries where cases with confirmed non-TB mycobacteria were not systematically reviewed and those judged non-TB were not de-notified; incomplete data on laboratory quality and high proportion of patients with no bacteriological confirmation of diagnosis are a potential source of error in estimates.

3.1.4 Method 4 - Notifications in high-income countries adjusted by a standard factor to account for under-reporting and under-diagnosis

TB surveillance systems from countries in the high-income group and other selected countries in the upper-middle income group are assumed to perform similarly well on average in terms of under-diagnosis and under-reporting. Exceptions include the Republic of Korea, where the under-reporting of TB cases has recently been measured using annual inventory studies and France, where the estimated level of under-reporting was communicated by public health authorities, based on unpublished survey results. In the United Kingdom and the Netherlands, incidence was obtained using capture-recapture modeling (see next section). Surveillance data in this group of countries are usually internally consistent. Consistency checks include detection of rapid fluctuations in notification rates and in the ratio of TB deaths / TB notifications (M/N ratio), which may be indicative of reporting problems. The standard adjustment, representing treatment coverage, applied for these countries was 85% (Uncertainty interval 75-100%).

3.1.5 Method 5 - Inventory studies, capture-recapture modelling

This method was used for 10 countries: China, Egypt [14], France, Germany, Indonesia, Iraq [15], the Netherlands [16], the Republic of Korea, the United Kingdom [17], and Yemen [18]. Capture-recapture modelling is considered in studies with at least 3 sources (lists) and estimation of between source dependences [9]. The surveillance gap (proportion of unreported incident cases) in the United Kingdom and the Netherlands was assumed time invariant. In Yemen, trends in incidence were derived from results of two consecutive tuberculin surveys. In Egypt, Indonesia

and Iraq, trends were derived using methods described in section describing method 1. Capture-recapture modelling for estimating TB incidence requires the following six assumptions: (i) all cases should be observable (preclinical stages are rarely detected before they become symptomatic); (ii) low proportion of mismatches and matching failures, which typically requires a large sampling fraction; (iii) closed population during the study period (typically 3-6 months); (iv) dependences between S data sources ($S \geq 3$) accounted for in the model design but S -way interaction assumed null - referrals between sources (e.g. clinic to lab) may imply an S -way interaction, invalidating the approach (of note, in many high-burden countries, there will not be 3 sources meeting requirements); (v) homogeneity of within-source observation probabilities across subpopulation groups such as defined by socio demographic characteristics; (vi) consistent case definitions across sources. It is anticipated that capture recapture may only be successfully implemented in very few high-burden countries planning an inventory study.

3.2 TB incidence in people living with HIV

Provider-initiated testing and counselling with at least 50% HIV testing coverage is the most widely available source of information on the prevalence of HIV in TB patients. However, this source of data is affected by selection biases, particularly when coverage is closer to 50% than to 100%. As coverage of HIV testing continues to increase globally, biases will decrease. Other sources of information on the prevalence of HIV among new TB cases include sero-surveys of a random sample of newly diagnosed TB cases and HIV sentinel surveillance systems when they include TB as a sentinel group. The different data sources were combined using local polynomial regression fitting by weighted least squares, using weight values of 1 for data from a nationally representative survey, 0.2 for data based on HIV sentinel surveillance, and a value equal to testing coverage in the case of data from provider-initiated HIV testing with coverage greater than 50%, and zero weights when testing coverage was less than 50%.

In countries with no surveillance data on HIV among TB cases, the prevalence of HIV was derived indirectly from the prevalence of HIV in the general population, based on the relationship between the prevalence of HIV in TB and the prevalence of HIV in the general population as follows: Let I and N denote incident cases and the total population, respectively, superscripts + and - denote HIV status, ϑ is the prevalence of HIV among new TB cases, h is the prevalence of HIV in the general population and ρ is the incidence rate ratio (people living with HIV over HIV-negative).

$$\rho = \frac{I^+/N^+}{I^-/N^-} > 1$$

$$\rho \frac{I^-}{I^+} = \frac{N^-}{N^+}$$

$$\rho \frac{I - I^+}{I^+} = \frac{N - N^+}{N^+}$$

$$\frac{I^+}{I} = \frac{\rho \frac{N^+}{N}}{1 + (\rho - 1) \frac{N^+}{N}} = \vartheta$$

$$\vartheta = \frac{h\rho}{1 + h(\rho - 1)}$$

The TB incidence rate ratio ρ can be estimated by fitting the following linear model with a slope constrained to 1

$$\log(\hat{\rho}) = \log\left(\frac{\vartheta}{1 - \vartheta}\right) - \log\left(\frac{h}{1 - h}\right), (\vartheta, h) \in]0, 1[$$

4. Mortality caused by TB, 2000–2019

The best sources of data about deaths from TB (excluding TB deaths among people living with HIV) are vital registration (VR) systems in which causes of death are coded according to ICD-10 (although the older ICD-9 and ICD-8 classification are still in use in several countries), using ICD-10: A15-A19 and B90 codes, equivalent to ICD-9: 010-018, and 137. When people with AIDS die from TB, HIV is registered as the underlying cause of death and TB is recorded as a contributory cause. Since one third of countries with VR systems only report to WHO the underlying causes of death and not contributory causes, VR data usually cannot be used to estimate the number of TB deaths in people living with HIV. Two methods were used to estimate TB mortality among HIV-negative people (see web content of WHO's *Global tuberculosis report 2024*):

- direct measurements of mortality from VR systems or mortality surveys;
- indirect estimates derived from multiplying estimates of TB incidence by estimates of the CFR.

4.1 Estimating TB mortality among HIV-negative people from vital registration data and mortality surveys up to 2019

As of July 2019, mortality data from 124 countries were used, representing 60% of the estimated number of TB deaths (among HIV-negative TB) globally in 2019.

Estimates for 15 countries, including South Africa (adjusted for HIV/TB miscoding), were obtained from the Institute of Health Metrics and Evaluation at <http://ghdx.healthdata.org/gbd-results-tool>, and readjusted to fit WHO mortality envelopes (the estimated number of deaths in total) by using a multiplication factor equal to the ratio of WHO to IHME envelopes.

Among the countries for which VR or mortality survey data could be used, which means that the coverage of the VR system is greater or equal to 60%, there were 1983 country-year data points 2000–2019 [19].

Reports of TB mortality are adjusted upwards to account for incomplete coverage (estimated deaths with no cause documented) and ill-defined causes of death (ICD-9: B46, ICD-10: R00–R99). It is assumed that the proportion of TB deaths among deaths not recorded by the VR system was

the same as the proportion of TB deaths in VR-recorded deaths. For VR-recorded deaths with ill-defined causes, it is assumed that the proportion of deaths attributable to TB is the same as the observed proportion in recorded deaths. The adjusted number of TB deaths κ_a is obtained from the VR report κ as follows:

$$\kappa_a = \frac{\kappa}{v(1 - g)}$$

where v denotes coverage (i.e. the number of deaths with a documented cause divided by the total number of estimated deaths) and g denotes the proportion of ill-defined causes. The uncertainty related to the adjustment was estimated as follows:

$$\hat{\sigma} = \frac{\kappa}{4} \left[\frac{1}{v(1 - g) - 1} \right]$$

The uncertainty calculation does not account for miscoding, such as HIV deaths miscoded as deaths due to TB, except in South Africa.

Missing data between existing adjusted data points are interpolated. Trailing missing values are predicted using a Kalman smoother or using the last observation carried forward or in the case of leading missing values, the next observation carried backwards.

In 2019, 60% of global TB mortality (excluding HIV) was directly measured from VR or survey data (or imputed from survey or VR data from previous years). The remaining mortality was estimated using the indirect methods described in the next section.

4.2 Estimates of the number of deaths caused by TB in India

From publication of the *Global tuberculosis report 2023* onwards, estimates of the annual number of deaths caused by TB in India have been based on new cause-of-death data from the country's sample registration system (SRS) for the period 2014–2019. Between February and April 2023, the Office of the Registrar-General and Census Commissioner of India published official reports of SRS cause-of-death data for the periods 2015–2017, 2016–2018 and 2017–2019. A report for the period 2014–2016 was published in May 2022. Reports for the periods 2004–2006, 2007–2009 and 2010–2013 were first published in September 2021. All these reports

are available for download on the website of the Office of the Registrar-General and Census Commissioner of India². Previously, there were no official reports in the public domain that included SRS cause-of-death data.

A quasi-binomial model was used to produce a complete time series of the proportion of deaths caused by TB for 2000–2019 (\widehat{p}_{TB}), based on officially-reported SRS raw values for multi-year time periods (with the raw value assigned to the mid-year). To produce estimates of the total number of deaths caused by TB (D_{TB}) for each year 2000–2019, the percentage of total deaths caused by TB was upward adjusted by a factor θ to allow for possible inaccuracies in VA-assigned cause of death as well as ill-defined causes, and then multiplied by WHO estimates of the total number of deaths in India (D).

$$D_{TB} = \frac{\widehat{p}_{TB} \times D}{\theta}$$

The upward adjustment was based on the values of SRS “raw” data as a proportion of GBD 2019 estimates in 2005, 2008 and 2012 (i.e. the years for which IHME has unpublished, detailed SRS datasets) and approximated as a uniform distribution with bounds of 0.70 and 0.85 (Table 4).

$$\theta \sim U_{[0.70, 0.85]}$$

² Office of the Registrar-General and Census Commissioner of India,
<https://censusindia.gov.in/census.website/data/SRSCOD>

Table 2 – Proportion of deaths caused by TB as reported by the SRS reports and IHME for 2005, 2008 and 2012.

| Year | GBD unadjusted % of deaths caused by TB SRS | GBD 2019 % of deaths caused by TB IHME | θ |
|-------------|--|---|----------------------------|
| 2005 | 5.10 | 5.90 | 0.85 |
| 2008 | 4.20 | 5.60 | 0.75 |
| 2012 | 3.60 | 5.20 | 0.70 |

4.3 Estimating TB mortality among HIV-negative people from estimates of case fatality rates and TB incidence

In countries lacking mortality data of the necessary coverage and quality, TB mortality is estimated as the product of TB incidence and the case fatality rate (CFR) after disaggregation by case type as shown in Table 3, following a literature review of CFRs by the TB Modelling and Analysis Consortium (TB-MAC):

$$M^- = (I^- - T^-)f_u^- + T^-f_t^- \quad (1)$$

where M denotes mortality, I incidence. f_u and f_t denote CFRs untreated and treated, respectively and the superscript denotes HIV status. T denotes the number of treated TB cases. In countries where the number of treated patients that are not notified (under-reporting) is known from an inventory study, the number of notified cases is adjusted upwards to estimate T^- accounting for under-reporting.

Table 3. Distribution of CFRs by case category

| | CFR | Sources |
|---------------------------|------------------|---------|
| Not on TB treatment f_u | 0.43 (0.28-0.53) | [21] |
| On TB treatment f_t | 0.03 (0-0.07) | [22] |

4.4 Estimating TB mortality among people living with HIV

TB mortality among people living with HIV is calculated exchanging superscripts - with + (Eq. 1). The case fatality ratios were obtained in collaboration with the TB Modeling and Analysis Consortium (TB-MAC) and are shown in Table 4. The disaggregation of incident TB into treated and not treated cases is based on the numbers of notified cases adjusted for under-reporting.

Direct measurements of HIV-associated TB mortality are urgently needed. This is especially the case for countries such as South Africa and Zimbabwe, where national VR systems are already in place. In other countries, more efforts are required to initiate the implementation of sample VR systems as an interim measure.

Table 4. Distribution of CFR in people living with HIV

| ART | TB treatment | CFR | Sources |
|------------|---------------------|------------------|--------------------------------|
| off | off | 0.78 (0.65-0.94) | [20] |
| off | on | 0.09 (0.03-0.15) | [22,23] |
| < 1 year | off | 0.62 (0.39-0.86) | Data from review + assumptions |
| < 1 year | on | 0.06 (0.01-0.13) | Data from review + assumptions |
| ≥ 1 year | off | 0.49 (0.31-0.70) | Assumptions |
| ≥ 1 year | on | 0.04 (0.00-0.10) | Assumptions |

5. Estimation of uncertainty, 2000–2019

There are many potential sources of uncertainty associated with estimates of TB incidence, prevalence and mortality, as well as estimates of the burden of HIV-associated TB and RR-TB. These include uncertainties in input data, in parameter values, in extrapolations used to impute missing data, and in the models used. Uncertainty in population estimates is not accounted for.

Notification data are of uneven quality. Cases may be under-reported (for example, missing quarterly reports from remote administrative areas are not uncommon), misclassified (in particular, misclassification of recurrent cases in the category of new cases is common), or over-reported as a result of duplicated entries in TB information systems or due to over-diagnosis. The latter issues can only be addressed efficiently in countries with case-based nationwide TB databases that include patient identifiers. Sudden changes in notifications over time are often the result of errors or inconsistencies in reporting.

Uncertainty bounds and ranges are defined as the 2.5th and 97.5th percentiles of outcome distributions. The general approach to uncertainty analyses is to propagate errors in m real-valued random variables X by approximating a function $h(X)$ using second-order Taylor series expansion about its moments.[24] Using matrix notation, the expected value $E[h(X)]$ and variance of $h(X)$ were approximated as follows:

$$E[h(X)] \approx h(E[X]) + \frac{1}{2!} tr H(h) \Sigma(X)$$

$$Var(h(X)) \approx \nabla(h) \Sigma(X) \nabla(h)^T + \frac{1}{2!} tr((H(h)) \Sigma(X))^2$$

where tr denotes the trace, $H(h)$ the Hessian matrix of partial second-order derivatives of $h(X)$ with respect to each $X_i=1..m$, $\nabla(h)$ the gradient matrix of partial first-order derivatives and $\Sigma(X)$ the joint covariance matrix of X .

6. Estimation of the impact of COVID-19 on the burden of TB, 2020–2023

Dynamical models were developed to produce estimates of TB incidence and mortality in 2020–2023 for certain countries. These new methods were required to produce estimates that account for the major disruptions to the provision of and access to TB diagnostic and treatment services that have occurred in the context of the COVID-19 pandemic. Compared to the methods used for the *2022 Global tuberculosis report*, this updated analysis includes: (i) a more streamlined modelling approach that allows, for example, modelling of countries that have *both* a large burden of HIV and a large private healthcare sector (ii) an updated list of countries modelled, (iii) an adjustment for under-reporting during COVID-19 disruptions and (iii) an updated approach for countries that were not individually modelled (region-specific models).

Estimates of TB incidence and mortality in all high-income countries in 2020–2023 were produced using the same methods as those used pre-2020; that is, notification data with a standard adjustment for incidence or inventory studies, and vital registration (VR) data for mortality. For low- and middle-income countries (LMIC) that were not modelled (i.e. those for which case notifications in 2020 and 2021 did not show a substantial reduction relative to pre-2020 trends), the methods used to estimate TB incidence and mortality before 2020 were retained for use in 2020–2023, with the assumption that pre-2020 trends continued in 2020–2023.

6.1 Country-specific dynamic models

The methodology was presented and reviewed at a meeting of a subgroup of the WHO Global Task Force on TB Impact Measurement in May 2022. More information is available in the background document prepared for the meeting and the meeting report [25].

Dynamic country-specific models were developed for 24 countries. These countries – prioritized based on the size of their contribution to the global shortfall in TB case notifications between 2019 and 2020/2021 – are listed in Table 5 below. Collectively, they accounted for 95% of the drop in global TB notifications from January 2020 to December 2022 inclusive. Countries for which pre-existing declining trends explained much of the decline in notifications in 2020 and 2021 were excluded (Ethiopia, Papua New Guinea and South Africa).

6.1.1 Model overview

Figure 2 shows a schematic illustration of the model. Although certain transitions (such as self-cure) are omitted for simplicity, the figure serves to illustrate a key component of the modelling approach: the time-varying rate of transition from undetected TB, to being on TB treatment. This rate incorporates all stages leading up to treatment initiation, i.e. the initial patient delay before first care seeking; any diagnostic delay before being successfully diagnosed with TB; and any treatment delay before successfully initiating treatment. Rather than aiming to model disruptions in each of these stages separately, the analysis concentrated on the total delay across all of these stages. The term $k(t)$ controls how this delay is shaped during periods of disruption. As described below, the value of $k(t)$ was adjusted on a month-by-month basis in order to reproduce the monthly time series of notifications from each country, from January 2020 onwards (or quarterly data from Q1 2020, where monthly is unavailable).

Figure 2. Schematic illustration of the model structure

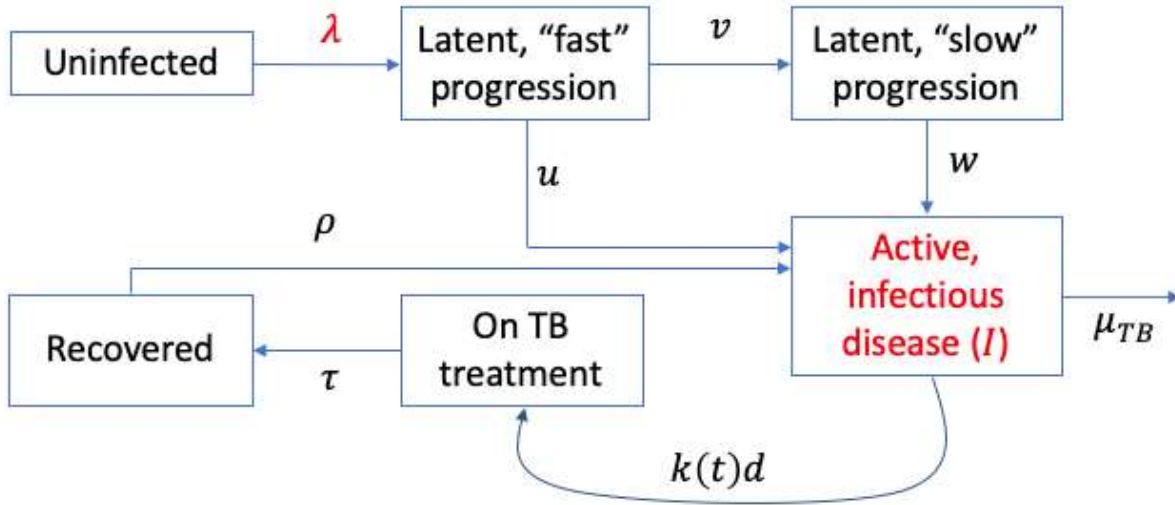


Figure 2 is a much-simplified version of the model, focusing on the key mechanism through which COVID-related disruptions are modelled (curved arrow at bottom of the figure). As described in the text, if pre-COVID rates of treatment initiation are given by the rate d , these rates were assumed to be modified by a time-dependent factor $k(t)$ during the pandemic, adjusted on a monthly (or quarterly) basis in order to match notification data. Additional model structure not shown, for simplicity, include the following: (i) The compartment 'On TB treatment' is split into two to represent public and private sectors, with respective rates of initiation on treatment labelled d_{pu} and

d_{pr} . (ii) All model compartments are divided into three strata to represent HIV status: HIV-negative, people living with HIV but not on ART; and on ART. (iii) 'Recovered' compartments are stratified into three types: recovered after treatment completion (with low relapse risk); after treatment interruption or self-cure (with high relapse risk); and long-term recovered (with minimal relapse risk). (iv) Other commonly incorporated transitions in TB natural history, not shown but present, include: self-cure, reinfection, and population turnover. See governing equations for the full model specification.

6.1.2 Model equations

The full model specification is as follows. In the following governing equations, the subscript h denotes HIV status, with values 0, 1, 2 denoting respectively: those who are HIV-negative, those with HIV but on ART; and those on ART. The subscript s denotes healthcare sectors, with values 0, 1 denoting respectively the public sector (including all non-public providers notifying TB), and the private (or non-notifying sector).

All state variables represent proportions of the population (rather than numbers). All model parameters are defined in Table 6. As described below, the function $f(.)$ in each equation denotes transitions between HIV strata in the model.

Uninfected (U):

$$\frac{dU_h}{dt} = b - \epsilon_h \lambda U_h - \mu_h U_h + f(U_h)$$

Latent 'fast' infection ($L_h^{(fast)}$):

$$\begin{aligned} \frac{dL_h^{(fast)}}{dt} = & \epsilon_h \lambda \left[U_h + (1 - c_h) \left(L_h^{(slow)} + R_h^{(lo)} + R_h^{(hi)} + R_h^{(st)} \right) \right] - (u_h + v_h + \mu_h) L_h^{(fast)} \\ & + f(L_h^{(fast)}) \end{aligned}$$

Latent 'slow' infection ($L_h^{(slow)}$):

$$\frac{dL_h^{(slow)}}{dt} = v_h L_h^{(fast)} - (w_h + \mu_h + \epsilon_h (1 - c_h) \lambda) L_h^{(slow)} + f(L_h^{(slow)})$$

Active, infectious disease (I_h):

$$\frac{dI_h}{dt} = u_h L_h^{(fast)} + w_h L_h^{(slow)} + \rho^{(lo)} R_h^{(lo)} + \rho^{(hi)} R_h^{(hi)} + \rho^{(st)} R_h^{(st)}$$

$$- \left[k(t)(d_{pu} + d_{pr} + g(t)) + \sigma_h + \mu_h^{(TB)} \right] I_h + f(I_h)$$

On TB treatment in sector s (T_{hs}):

$$s = 0: \frac{dT_{h,0}}{dt} = k(t)d_0I_h + k(t)g(t)I_h - \left(\tau + \delta + \mu_h^{(TB)} \right) T_{h,0} + f(T_{h,0})$$

$$s = 1: \frac{dT_{h,1}}{dt} = k(t)d_1I_h - \left(\tau + \delta + \mu_h^{(TB)} \right) T_{h,1} + f(T_{h,1})$$

Recovered, with high risk of relapse (self-cure or following treatment interruption):

$$\frac{dR_h^{(hi)}}{dt} = \sigma_h I_h + \delta T_{hs} - \left(\rho^{(hi)} + r + \mu_h + \epsilon_h(1 - c_h)\lambda \right) R_h^{(hi)} + f(R_h^{(hi)})$$

Recovered, with low risk of relapse (following treatment completion):

$$\frac{dR_h^{(lo)}}{dt} = \tau T_{hs} - \left(\rho^{(lo)} + r + \mu_h + \epsilon_h(1 - c_h)\lambda \right) R_h^{(lo)} + f(R_h^{(lo)})$$

Recovered, long-term stabilized relapse risk:

$$\frac{dR_h^{(st)}}{dt} = rR_h^{(hi)} + rR_h^{(lo)} - \left(\rho^{(st)} + \mu_h + \epsilon_h(1 - c_h)\lambda \right) R_h^{(st)} + f(R_h^{(st)})$$

Force-of-infection (λ):

$$\lambda = \sum_h \beta_h I_h$$

where β_h is the rate-of-infection associated with TB disease with HIV status h . Because HIV positive TB can be less infectious than HIV-negative TB, β_1 is expected to be lower in value than β_0 and β_2 . Accordingly, it was assumed that $\beta_0 = \beta_2 = m\beta_1$, for a parameter m to be calibrated, and constrained to be between 0 and 1.

In all the above equations, $f(\cdot)$ denotes transitions between HIV states. For any given state variable X_h , it is defined as follows:

$$f(X_h) = \begin{cases} -r_{HIV}X_0 & \text{if } h = 0 \\ r_{HIV}X_0 - r_{ART}X_1 & \text{if } h = 1 \\ r_{ART}X_1 & \text{if } h = 2 \end{cases}$$

where r_{HIV} denotes the per-capita rate of acquiring HIV, and r_{ART} denotes the per-capita rate of initiating ART.

Notifications in a time interval τ (for example, a month) are calculated using:

$$\int_{\tau} \left[k(t) d_{pu} \sum_h I_h \right] dt$$

Finally, for simplicity the birth rate b was chosen to maintain a constant population size, i.e.

$$b = \sum_h \mu_h \left[U_h + L_h^{(fast)} + L_h^{(slow)} + T_{h0} + T_{h1} + R_h^{(lo)} + R_h^{(hi)} + R_h^{(st)} \right] + \mu_h^{(TB)} I_h$$

6.1.3 Implementation

The model captures both HIV/TB coinfection, and settings where the private sector plays a strong role in the management of TB. In implementation, only the HIV/TB structure was used in countries where individuals with HIV accounted for at least 10% of TB incidence, in 2019. The public/private structure was used for countries belonging to the WHO PPM priority list (see ref. [26]), as well as countries from the WHO South-East Asia region having private sectors that are not part of this list. Table 5 lists countries by the model structure employed.

Table 5. List of countries modelled, and the model structures employed

| HIV/TB | Public/private | HIV/TB and public/private | Neither HIV/TB nor public/private |
|--|--|---------------------------|--|
| Brazil ^a Colombia Lesotho Zimbabwe | Angola Bangladesh ^b Cambodia India Indonesia Myanmar Nepal Pakistan Philippines Viet Nam | Kenya Thailand | Afghanistan Azerbaijan ^a Kazakhstan ^a Kyrgyzstan Malaysia Mexico Mongolia ^c Peru Ukraine ^a |

^a TB mortality was estimated using vital registration data for 2020-2023

^b Incidence was estimated using prevalence survey

^c These countries were selected for the regional model but were the sole countries in their respective regions (and hence were included in the list of countries for country-level modelling).

For countries where the HIV/TB structure is not needed, the parameters β_h, u_h, v_h, w_h were all set equal to zero for $h \in [1,2]$, as well as parameters r_{HIV} and r_{ART} . For countries where the public/private structure is not needed, the parameter d_{pr} was set equal to zero.

To implement the model for a given set of parameters θ , a perturbation to a disease-free equilibrium was first modelled, then simulating to endemic equilibrium. To account for programmatic and HIV-related factors that drive non-equilibrium trends in TB burden, the following approaches were adopted with the different model structures:

HIV/TB structure: The equilibrium phase of the simulation assumed no HIV and no ART. Starting from 1980, the introduction of HIV was then modelled by incorporating data for annual HIV incidence (through r_{HIV}). For simplicity ART scale-up (through r_{ART}) was approximated in a linear way, calibrating the per-capita rate of ART initiation in 2019 in order to match ART coverage in that year. Conservatively, it was assumed that there were no disruptions to HIV services during COVID-related lockdowns.

Public/private structure: The equilibrium phase of the simulation assumed no public TB services (i.e. $d_{pu} = 0$), consistent with conditions prior to the DOTS strategy (see e.g. Mandal et al, 2017 [27]). The introduction of nationally coordinated TB services was then modelled by assuming a linear scale-up of d_{pu} from 0 to its value in θ , over the period from 2000 to 2009.

All other countries: While the changes described above provide a mechanistic basis for trends in each of the modelled countries, they are not applicable in settings such as the Russian Federation. Here, declines in TB burden are more likely due a large recent expansion in screening for TB, resulting in an increase in case-finding. Consistent with these changes, for such countries - without substantial burden of HIV nor a sizeable private healthcare sector - the model incorporated a per-capita rate of 'case-finding' g , assumed to scale up linearly from 0 to its value in θ , over the period from 2014 to 2019.

6.1.4 Data and calibration

The following WHO estimates from 2019 were used for different country categories:

Countries with high HIV/TB burden:

- Estimated incidence and mortality rates of HIV-negative TB in 2019, with uncertainty intervals
- Estimated incidence and mortality rates of TB in people with HIV TB in 2019, with uncertainty intervals
- Notification rate (all TB) in 2019
- Proportion of PLHIV on ART, all years up to 2019
- Prevalence of HIV, all years up to 2019

Countries with private sector:

- Estimated incidence and mortality in 2019, with uncertainty intervals
- Notifications in 2019

All other countries:

- Estimated incidence and mortality in 2014, with uncertainty intervals
- Estimated incidence and mortality in 2019, with uncertainty intervals
- Notifications in 2019

For each calibration target, beta distributions were fitted for proportions, and log-normal distributions for all other data; an overall log-likelihood term was then defined as the summation of the log-likelihoods corresponding to each relevant data element. Uniform distributions were mostly assumed for prior distributions for each of the parameter ranges shown in Table 6. One exception was in the case of countries with a private sector, where a prior beta distribution was posed for the proportion contribution of the public sector, to the overall numbers of TB patients receiving treatment. Without this constraint, certain country models can assign implausibly high values to either d_{pu} or d_{pr} , so that the private sector handles either a negligible minority or an overwhelming majority of TB treatment. A relatively broad prior was chosen for the proportion of TB treatment managed by the public sector, assuming 95% uncertainty intervals of 30% - 70%.

Markov-Chain Monte Carlo was used to sample from the posterior density, using adaptive MCMC [28] to efficiently determine the covariate structure for the proposal distribution. For all model outputs, uncertainty intervals were estimated by evaluating the 2.5th, 50th and 97.5th percentiles of the posterior distribution.

6.1.5 Modelling disruptions to TB services

The analysis concentrated on delays to diagnosis and treatment initiation, ignoring disruptions to treatment continuity amongst those already on TB treatment, partly for lack of systematic data, but also because previous modelling analysis [29] suggests that these types of disruptions are likely to have a weaker effect on incidence, than disruptions to diagnosis and treatment initiation.

The intensity and duration of disruptions was informed by monthly notifications (quarterly where monthly data is unavailable), as reported to WHO. It was assumed that any reduction in notifications, compared to an extrapolation of pre-2020 trends, arises from delays to diagnosis and treatment initiations, rather than shortfalls in reporting. In turn, these delays may arise from patient-related factors (e.g. symptomatic patients being less willing or able to seek care during periods of anti-COVID restrictions), or from health system related factors (e.g. TB programmes having less diagnostic capacity or human resources than usual times). The model structure shown above is agnostic to either of these factors, as the whole patient care seeking journey is made implicit in the rates of treatment initiation, shown as d_{pu} in figure 1.

Assuming that treatment initiations are a reasonable proxy for notifications, the number of notifications in each month n is:

$$n = \sum_h \left[\int_n^{\{n+1\}} k(t) d_{pu} I_h dt \right],$$

where I_h is the number of individuals having active, infectious disease in Figure 1, with HIV status h . Using the full transmission model, the monthly value of $k(t)$ was therefore adjusted in such a way as to yield treatment initiations consistent with the monthly notification data. The timeseries for $k(t)$ determined in this way, then formed the basis for model projections for incidence.

Lockdown-related reductions in TB transmission

As much as lockdowns and social restrictions can control transmission of COVID-19, they may also have had similar effects on TB transmission. It was assumed that in any setting experiencing a country-wide lockdown, there was a temporary, $x\%$ reduction in TB transmission during that period of lockdown (with transmission returning to pre-lockdown levels as soon as restrictions were lifted). Given uncertainty about the strength of these effects in different settings, x was drawn from a uniform probability distribution over the interval [25,75]. For any country implementing subnational lockdowns, this reduction was scaled in proportion to the share of the country's population undergoing those lockdowns.

Allowing for under-reporting

Most countries that showed reduced notifications during the COVID-19 pandemic also showed a subsequent increase in notifications, temporarily exceeding pre-pandemic levels, as TB services recovered and met the backlog of undiagnosed TB. However, certain countries did not show such a temporary 'excess' of notifications, including some countries where notifications apparently have still not returned to pre-pandemic levels. In such countries, in order to reconcile notification data with evidence from the respective TB programmes that services had in fact returned to pre-pandemic levels, some of the reduction in notifications was attributed to under-reporting, rather than under-diagnosis. The extent of under-reporting was determined in order for model-inferred disruptions to TB services to return to zero by the end of 2022 and ranged from 10 – 20% for the countries in which this adjustment was applied.

Aligning model projections with WHO uncertainty intervals

Because model projections are presented as a continuation of pre-2020 WHO estimates, there is a need to ensure continuity with at least point and uncertainty intervals in 2019. This continuity does not necessarily occur automatically because by its nature, the model makes mechanistic links between incidence, mortality and other calibration targets. Thus, model-based posterior distributions for calibration targets can be narrower than the inputs provided by WHO estimates. Model-based uncertainty was inflated to ensure alignment of uncertainty intervals between WHO and model estimates in 2019, for all calibration targets.

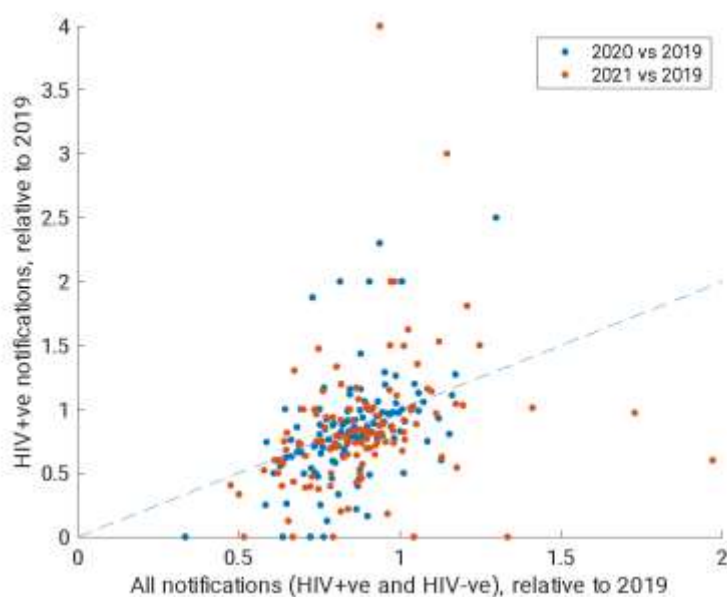
6.1.6 Model limitations

As with all models, this analysis has some important limitations to note. Principally, it was assumed that drops in notifications can be attributed entirely to delays to diagnosis and treatment initiation. Other mechanisms may also operate, including reductions in TB transmission. While the modelling allows for such reductions during periods of lockdown and other restrictions, it does address the potential for sustained reductions, for example as a result of greater mask use, even after restrictions were lifted. Given the slow nature of TB transmission

dynamics, any such transmission effects would be expected to manifest fully on the order of years, rather than months.

This analysis also makes a range of simplifying assumptions: other possible types of service disruptions were ignored, including to preventive therapy, and to continuity of TB treatment. Sub-annual notification data is provided aggregated across all age groups, and so it is not possible to model differential disruptions by age. It was also not possible to model differential disruptions by HIV status. For example, it might be hypothesized that those already in HIV care may be more less likely to experience disruptions, given that they are already engaged in the healthcare system. However, analysis of annual data from 2020–2023 suggests that PLHIV did not systematically see less pronounced disruptions in TB diagnosis, than those without HIV (Figure 3). Finally, while this analysis focuses on TB services, it also ignores the potential adverse impact of the pandemic on broader TB determinants, such as undernutrition and poverty. Such factors may contribute still further to long-term increases in TB burden.

Figure 3. Comparison of disruptions in TB notifications among people with HIV alone (vertical axis), vs all TB notifications (horizontal axis)



In Figure 3, ‘disruptions’ are quantified simply as the ratio of notifications in 2020 or 2021, vs those in 2019. Each point represents a country where HIV coinfection accounts for >10% of TB incidence. These comparisons are

performed on annual data because subannual data is not stratified by HIV status. The diagonal dashed line shows the level where disruptions felt by people living with HIV disruptions would be equivalent to overall disruptions; if the former were systematically less severe, then most points would lie below this line. However, as illustrated by the figure, there appears to be no systematic bias in either direction.

Table 6. Definitions and values of model parameters

| Symbol | Definition | | Value (range) | Source |
|---------------------------|--|--|--|--|
| <i>TB natural history</i> | | | | |
| β_h | Average annual infections per TB case | $h = 0$ (HIV -ve) | Calibrated to match epidemiological data, with uniform priors [0 - 30] | |
| | | $h = 1$ (HIV+ve, not on ART) $h = 2$ (on ART) | | |
| u_h | Per-capita annual rate of progression to active TB from 'fast' latent infection | $h = 0$ (HIV -ve) | 0.0826 (0.041, 0.12) | Menzies (2018)[30], with uniform prior using intervals of $\pm 50\%$ |
| | | $h = 1$ (HIV+ve, not on ART) | $u_1 = k_{LTBI}u_0$, for k_{LTBI} to be calibrated to match HIV/TB incidence, with uniform ranges of [1 - 100] | |
| | | $h = 2$ (on ART) | $u_2 = u_1(0.4 - 0.24p)$, where p is the coverage of IPT amongst those on ART, and assuming that ART and IPT independently have 60% effectiveness in reducing TB incidence. Formula derived as a weighted average (weighted by p) of progression rates depending on TPT status | |
| v_h | Per-capita annual rate of stabilisation from latent 'fast' to latent 'slow' compartments | $h = 0$ (HIV -ve), $h = 2$ (on ART) | 0.872 (0.44 – 1.3) | Menzies (2018)[30], with uniform prior using intervals of $\pm 50\%$ |
| | | $h = 1$ (HIV+ve, not on ART) | 0 | |

| | | | | |
|----------------|--|--|--|--|
| w_h | Per-capita annual rate of reactivation to active TB from 'slow' latent infection | $h = 0$ (HIV -ve) | 6×10^{-4} (3×10^{-4} $- 9 \times 10^{-4}$) | Menzies (2018)[30], with uniform prior using intervals of $\pm 50\%$ |
| | | $h = 1$ (HIV +ve, not on ART) | $w_1 = k_{LTBI}w_0$, for k_{LTBI} to be calibrated to match HIV/TB incidence, with uniform ranges [1 - 100] | |
| | | $h = 2$ (on ART) | $w_2 = w_1(0.4 - 0.24p)$, where p is the coverage of IPT amongst those on ART, and assuming that ART and IPT independently have 60% effectiveness in reducing TB incidence | |
| $\mu_h^{(TB)}$ | Per-capita annual rate of mortality, untreated TB | $h = 0$ (HIV -ve), $h = 2$ (on ART) | 1/6 (0.083, 0.25) | Tiemersma (2011)[21], with uniform prior using intervals of $\pm 50\%$ |
| | | $h = 1$ (HIV+ve, not on ART) | $k_{mort} \cdot \mu_0^{(TB)}$, for parameter k_{mort} calibrated to match HIV/TB mortality, with uniform ranges [1 – 10] | |
| σ_h | Per-capita annual rate of spontaneous recovery | $h = 0$ (HIV -ve), $h = 2$ (on ART) | 1/6 (0.083, 0.25) | Tiemersma (2011)[21], with uniform prior using intervals of $\pm 50\%$ |
| | | $h = 1$ (HIV+ve, not on ART) | 0 | Assumption |
| c_h | Protection from reinfection arising from prior exposure | $h = 0$ (HIV -ve), $h = 2$ (on ART) | [0.5 – 0.9] | Andrews (2012) [31], with uniform prior across range shown |
| | | $h = 1$ (HIV+ve, not on ART) | 0 | Assumption |
| ϵ_h | Relative exposure to TB amongst those having HIV | $h = 0$ (HIV -ve) | 1 (Reference) | |
| | | $h = 1$ (HIV+ve, not on ART) | [0 – 10] | Calibrated, with uniform prior across range shown |
| | | $h = 2$ (on ART) | | |

| | | | | |
|--------------------------------|--|--|--|---|
| <i>Treatment and post-cure</i> | | | | |
| d_{pu} | Per-capita annual rate of diagnosis and treatment initiation in the public sector, including all private providers notifying TB | | Calibrated to match notification data | |
| d_{pr} | Per-capita annual rate of diagnosis and treatment initiation in the private (non-notifying) sector | | Calibrated with prior on proportion of TB treatment provided by private sector (i.e. $d_{pr}/(d_{pr} + d_{pu})$) having beta distribution with 2.5 th , 97.5 th percentiles respectively 0.3 and 0.7 | |
| $g(t)$ | Per-capita annual rate of linkage to treatment, as a result of case-finding efforts (non-HIV, non-private sector countries only) | | Incorporated to provide mechanistic basis for trends in countries without HIV or private sector. The parameter g is assumed to increase in a linear way from 0 in 2014, to a value g_{max} in 2019. The value of g_{max} is calibrated to match incidence in 2014 and 2019, with uniform prior with range [0 – 10] | |
| $k(t)$ | COVID-induced reductions in rate of diagnosis and treatment initiation | | Monthly (or quarterly) time series determined to match notification data | |
| τ | Per-capita annual rate of first-line treatment completion | | 2 | Corresponding to standard treatment duration of 6 months |
| δ | Per-capita annual rate of treatment interruption | | Adjusted to match treatment completion rates | Country programme data |
| $\rho^{(lo)}$ | Per-capita annual rate of relapse in first two years after treatment completion | | 0.032 (0.016 – 0.048) | Romanowski (2019)[32], Menzies (2009)[33] and Weis (1994)[34], with uniform prior using intervals of $\pm 50\%$ |
| $\rho^{(hi)}$ | Per-capita annual rate of relapse in first two years after self-cure or incomplete treatment | | 0.14 (0.07 – 0.21) | |
| $\rho^{(st)}$ | Per-capita annual rate of relapse >two years after last TB episode | | 0.0015 | |
| r | Per-capita annual rate of ‘stabilising’ from high to low relapse risk | | 0.5 | Most relapse occurs in first two years after recovery: |

| | | | | |
|---------------------|---|--|------------------------------------|--|
| | | | | Guerra-Assuncao (2015)[35] |
| <i>Demographics</i> | | | | |
| μ_h | Per-capita background annual mortality hazard, in absence of TB | $h = 0$ (HIV -ve), $h = 2$ (on ART) | 1/Mean lifespan | |
| | | $h = 1$ (HIV+ve, not on ART) | Calibrated to yield HIV prevalence | HIV prevalence estimates from Thembisa model[36] |

6.2 Region-specific dynamic models

In addition to the 24 countries listed in Table 5, there were several countries that had seen substantial disruptions, but did not contribute sufficiently to the global burden to be incorporated into the country-specific modelling. These 23 countries were modelled at the level of their respective WHO regions, as follows.

Countries selected for the regional modelling were those fulfilling the following criteria: (i) non-high-income countries that were not included in Table 5, and (ii) that saw >10% reductions in notifications in 2020 and 2021 compared to 2019. Countries were excluded if these reductions could be explained by an extension of pre-2020 trends (this was the case for Georgia only). Table 7 below lists these countries, and the WHO regions to which they belong.

For each region, all country data were aggregated to the regional level weighted by population size. The modelling described above was then applied to each region, to capture incidence and mortality projections at the regional level. Finally, to create country-level projections, it was assumed that incidence in year t , relative to that in 2019, was the same for a given region as for all countries within that Region. Thus model-based incidence projections at the regional level were extrapolated to the country level, and similarly for mortality projections.

Table 7. Countries modelled as regional aggregations, by WHO region

| Africa | The Americas | Europe |
|---------------------------------|---|--|
| Botswana Eswatini Namibia | Argentina Belize Bolivia (Plurinational State of) Costa Rica Cuba Dominican Republic Ecuador Grenada Guatemala Honduras Jamaica Nicaragua Paraguay Suriname ^a Venezuela (Bolivian Republic of) | Albania Armenia Belarus Montenegro Republic of Moldova Tajikistan |

^a Incidence was estimated using case notification data with standard adjustment

7. Disaggregation of TB incidence and mortality by age and sex, 2023

The methods used for estimating tuberculosis incidence and mortality by age and sex were previously published [37] and are presented in this section.

7.1 TB incidence

Estimates for men (males aged ≥ 15 years), women (females aged ≥ 15 years) and children (aged < 15 years) are derived as follows. Age and sex disaggregation of smear-positive TB case notifications has been requested from countries since the establishment of the data collection system in 1995, but with few countries reporting these data to WHO. In 2006, the data collection system was revised to additionally monitor age-disaggregated notifications for smear-negative and extrapulmonary TB. The revision also included a further disaggregation of the 0–14 age group category to differentiate very young children (0–4 years) from older children (5–14 years). While reporting of age-disaggregated data was limited in the early years of the data collection system, reporting coverage continued to improve. For 2012 case notifications, age-specific data reached 99%, 83% and 83% of total smear-positive, smear-negative and extrapulmonary tuberculosis global case notifications, respectively. Finally in 2013, another revision of the recording and reporting system was necessary to allow for the capture of cases diagnosed using WHO-approved rapid diagnostic tests (such as Xpert MTB/RIF) [38]. This current revision requests the reporting of all new and relapse case notifications by age and sex.

While there are some nationwide surveys that have quantified the amount of under-reporting of cases diagnosed in the health sector outside the network of the NTPs [14,16,39] none have produced precise results by age. Small-scale, convenience-sample studies indicate that under-reporting of childhood TB can be very high [40,41] but extrapolation to national and global levels has not yet been possible. Producing estimates of TB incidence among children remains challenging primarily due to diagnostic challenges and the lack of age-specific, nationwide, robust survey and surveillance data.

In order to maintain consistency with total TB incidence and its uncertainty, the approach to estimating TB incidence by age and sex sought to disaggregate total incidence into incidence for each age group and sex. For countries where incidence was based on either a capture-recapture study or a standard factor adjustment of notification, and the implied case detection ratio was over 85%, we disaggregated total TB incidence by age and sex in proportion to case notifications. For these countries, surveillance systems were assumed to function well enough to inform patterns by age and sex directly. We also disaggregated incidence in proportion to case notifications in countries where fewer than 1,000 TB cases were reported in total. In these countries, there may be marked variability and modelled estimates are less appropriate.

For other countries, one million samples were drawn from a country 'prior' for the proportion of incidence in each age and sex group. Samples were accepted if they resulted in incidence exceeding notifications in every age and sex category. Where no samples were accepted, the 100 samples with the smallest undershoot were accepted. Final incidence estimates were based on the mean over accepted samples.

The prior for each country for adults was based on a hierarchical analysis for prevalence risk ratios which was developed based on TB prevalence survey data and Horton et al's systematic review of prevalence sex ratios [42]. This prior closely followed age and sex patterns for TB prevalence in countries with surveys, and made predictions (with greater uncertainty) for countries without prevalence surveys. The prior for children was based on a mathematical modelling approach that simulates the course of natural history of TB in children, starting from estimates of TB infection in children as a function of demographic and adult TB prevalence, and subsequently modelling the progression to pulmonary and extra-pulmonary TB disease taking into account country-level BCG vaccination coverage and HIV prevalence [43]. The disaggregation by sex in children was based on a random-effects meta-analysis of the sex ratio in notification data for children (0-14 years).

Finally, for a small number of countries the approach above generated results that lacked face validity and a standard adjustment factor was applied to notifications instead.

7.2 TB mortality

TB mortality is disaggregated by age and sex using the age- and sex-specific adjusted (for coverage and ill-defined causes) number of deaths from VR data in countries with high-quality vital registration systems in place (ie, where these data have been used to estimate the TB mortality envelope) [37]. For other countries, adult mortality is disaggregated by age, sex and HIV-infection status by applying CFRs to disaggregated incidence estimates, distinguishing CFR by anti-TB treatment status and HIV/ART status (see Tables 2 and 3). TB mortality in children for these countries is also estimated from TB incidence in children using a case-fatality based approach [44]. This approach distinguishes case fatality in children by age, anti-TB treatment status, and HIV/ART status. TB deaths in adults living with HIV are distributed by age and sex proportional to age- and sex-specific HIV prevalence from UNAIDS estimates in such a way as to maintain the estimated total number of TB deaths amongst people living with HIV.

8. Drug-resistant TB - incidence and proportions with resistance

8.1 Proportions of new and previously treated TB cases with rifampicin resistance

Previous WHO Global TB Reports included estimates of drug resistance for the latest calendar year only. New methods were developed in 2022 and allow the production of time series of estimates for the period 2015–2023. The time series are for the proportions of TB cases (new and previously treated) that have rifampicin-resistant (RR) TB and the absolute number of incident RR-TB cases, of which multidrug-resistant (MDR) TB is a subset. The methodology was presented and reviewed at a meeting of a subgroup of the WHO Global Task Force on TB Impact Measurement in May 2022. More information is available in the background document prepared for the meeting and the meeting report [25].

All surveys conducted according to WHO guidance[45] as well as all routine surveillance data meeting quality thresholds from 2000-2023 were used to inform the model. For routine surveillance data to be considered representative for new patients, two criteria must be met: (i) at least 80% of notified new pulmonary bacteriologically-confirmed TB cases must have a documented drug susceptibility testing result for at least rifampicin, and (ii) the proportion of pulmonary bacteriologically-confirmed cases having unknown previous treatment history must be no more than 25%. For data from routine surveillance to be considered representative for previously treated patients, at least 80% of notified retreatment pulmonary bacteriologically-confirmed TB cases must have a documented drug susceptibility testing result for at least rifampicin.

Briefly, hierarchical regression models within a Bayesian paradigm were considered, and the best performing model selected for use. The data likelihood treats surveillance data as multinomial count data; estimates of RR-TB prevalence among TB cases derived from surveys are considered to be distributed log-normal with known precision.

Models consider intercept and linear trends on an abstract space that is mapped to the observed prevalences of resistance using a softmax transformation. Intercepts and trends are modelled through multivariate regressions for each patient group (new and previously treated), with

regions used as covariates (the regions used are the six WHO regions plus a grouping of the former republics of the Soviet Union, totaling 7 categories). The modelling choices explored related to the approach for modelling random effects (i.e. the hierarchical elements), with the final model using Leroux conditional autoregressive priors for both the intercept and trend, separately for new and retreatment patients. This class of model makes use of a spatial structure, with estimates for neighboring countries with imprecise or missing data being more strongly informed by nearby countries than distant ones. Models were fitted with MCMC using Stan [46].

The models estimate the prevalence of resistance for 215 countries and territories for the years 2015-2023. The hierarchical nature of these models means that the learned distributions of random effects together with regression covariates (time and region) allow predictions of prevalence to be made for country-years without data, and for the uncertainty of estimates to respond to data, but with some degree of smoothing over temporal fluctuations. The selected model will be refitted over all years of data in future estimation rounds, generating revised estimates for the whole time series of prevalence estimates.

8.2 Incidence of RR-TB

To estimate the incidence of MDR/RR-TB, the same approach as previous years was adapted to include the time-dependence in the estimated proportions of new ($p_n(t)$) and retreated ($p_r(t)$) patients with MDR/RR-TB:

1. Estimate the proportion r of relapses out of the sum of new and relapse cases;
2. Estimate f the cumulative risk for incident cases to receive a non-relapse retreatment (retreatment following previous treatment failure or return after default);
3. Approximate RR incidence as:

$$I_{rr}(t) = I(t) \left[(1 - f)p_n(t)((1 - r) + r\rho) + fp_r(t) \right]$$

where t is the year, $I(t)$ is total TB incidence, and ρ is the risk of MDR/RR-TB in relapses relative to previously untreated cases.

f may be estimated based on reported counts of cases disaggregated by treatment history over the most recent years.

8.3 Proportion of RR-TB cases with resistance to fluoroquinolones (pre-XDR-TB)

All surveys conducted according to WHO guidance as well as all routine surveillance data meeting quality thresholds from the previous 15 years (2007-2023) were used. For data from routine surveillance to be considered representative for fluoroquinolone resistance among MDR/RR-TB patients, the two criteria described above for rifampicin must be met. Additionally, at least 80% of MDR/RR-TB cases must have a documented drug susceptibility testing result for at least one fluoroquinolone. The average proportion of MDR/RR-TB cases with fluoroquinolone resistance is calculated by taking the ratio of identified fluoroquinolone-resistant cases among tested MDR/RR-TB cases. Errors are assumed to be binomial. The proportions of fluoroquinolone resistance were then pooled using country-specific estimates of MDR/RR-TB incidence as weights to generate a global estimate.

9. Drug-resistant TB - mortality

The VR mortality data reported to WHO by Member States do not differentiate between drug-resistant and drug-susceptible TB as a cause of death (there is no specific ICD-9 or ICD-10 codes for MDR/RR-TB, although some countries such as South Africa have allocated two specific codes U51 and U52 to classify deaths from MDR-TB and XDR-TB respectively) [47]. Therefore, a systematic review and meta-analysis of the published literature was undertaken to estimate the odds ratio of dying from MDR-TB compared with non MDR-TB. We are assuming this odds ratio of death is the same as that for RR-TB. The global estimate of MDR/RR-TB deaths is based on the following formula:

$$m = \frac{Mpr}{(1 - p + pr)}$$

Where:

m = global MDR/RR-TB mortality,

M = global TB mortality,

p = overall proportion of MDR/RR-TB among prevalent TB cases, approximated by the weighted average of the proportion of new and retreated cases that have MDR/RR-TB,

r = the odds ratio of dying from MDR/RR-TB versus non-MDR/RR-TB.

10. Deaths averted by TB interventions

To estimate the number of deaths averted by TB interventions from 2010-2023, the actual numbers of TB deaths can be compared with the number of TB deaths that would have occurred in the absence of TB treatment (and without ART provided alongside TB treatment for people living with HIV). The latter number can be estimated conservatively as the number of estimated incident cases multiplied by the relevant estimated CFR for untreated TB. The CFR is calculated based on the combined total of deaths in HIV-negative and people living with HIV for the purpose of cross-country comparisons; in particular, to illustrate the high CFRs in African countries, which could be reduced by effective detection and care programmes. CFRs restricted to HIV-negative TB deaths and cases can also be calculated but are not shown here. At the subnational level, CFRs can also be restricted to HIV-negative TB deaths, depending on the country and its HIV burden.

The estimate of the number of deaths averted is conservative because it does not account for the impact of TB services or availability of ART on the level of TB incidence; it also does not account for the indirect, downstream impact of these interventions on future levels of infections, cases and deaths.

11. Household contacts of bacteriologically confirmed pulmonary TB eligible for TB preventive therapy (TPT)

In low TB burden countries, the number of household contacts aged under 5 years and eligible for TPT is defined as the number of children aged under 5 years who are household contacts of bacteriologically confirmed pulmonary TB cases and who have a positive result to testing for TB infection. In high TB burden countries, the number eligible is defined as the number of children under 5 years of age who are household contacts of bacteriologically confirmed pulmonary TB cases and who are not found to have active TB on appropriate clinical evaluation, without the requirement to test for TB infection [48,49].

The estimated number n_{u5} of household contacts aged under 5 years and eligible for TPT is

$$n_{u5} = \frac{b}{c}HpL(1 - t)$$

The estimated number n of household contacts of all ages eligible for TPT is

$$n = \frac{b}{c}(H - c)$$

See **Table 8** for details of the equation parameters and sources.

The following sources of uncertainty are accounted for: prevalence of TB infection, variance in the number of TB cases per household, and variance in the proportion of household contacts aged under 5 years with active TB. Uncertainty about United Nations Population Division (UNPD) population size is not documented. Errors were propagated using methods described in Chapter 5.

Table 8. Parameters and sources

| Symbol | Parameter | Values | Sources |
|--------|---|--|---|
| b | Number of notified bacteriologically confirmed pulmonary TB in 2021 | Differ by country | WHO global TB database |
| p | National proportion of children aged <5 years in 2022 | Differ by country | 2022 Revision of World Population, United Nations Population Division (https://esa.un.org/unpd/wpp/) |
| H | National average household size | Differ by country | National censuses, DHS statistical year books, or official websites of the national statistical authorities |
| L | Prevalence of TB infection among child household contacts aged <5years in LBC | Constant across countries = 27.6% (19.2%-38.0%) In high TB burden countries, L is set to 1 (testing for TB infection is not required) | Systematic review of literature from LBC up to Dec 2015 (unpublished) |
| c | Average cluster size of active TB per household | Constant across countries =1.06 (95%CI 1.04-1.08) | Systematic review of literature between Jan 2005 and Dec 2015 (unpublished) |
| t | Proportion of children aged <5 years with active TB among those who had a household contact with TB cases | Constant across countries =6.1% (95%CI 1.0%-16.3%) | Dodd et al, Lancet Glob Health. 2014[43] |

12. Excess number of deaths caused by TB during the COVID-19 pandemic and its aftermath, 2020–2023

The excess number of deaths caused by TB during the COVID-19 pandemic was estimated as the cumulative difference in the number of deaths caused by TB as estimated in the *Global tuberculosis report 2024* and the counterfactual of the estimated number of deaths that would have been caused by TB in the absence of the COVID-19 pandemic.

The counterfactual of the estimated number of deaths that would have been caused by TB in the absence of the COVID-19 pandemic was estimated assuming that the decline in the number of deaths caused by TB before the COVID-19 pandemic remained similar in the period 2020–2023. A quasi-binomial regression was fitted to capture the trend in the estimated number of deaths caused by TB in the period 2017–2019, and estimated parameters were used to project the counterfactual of the estimated number of deaths that would have been caused by TB in the absence of the COVID-19 pandemic.

The resulting projections were shown in Figure 1.2.2 of the web content of the *Global tuberculosis report 2024* and suggested an estimated +676,648 deaths caused by TB (95%UI 187,107 – 1,189,162).

13. Attributable risk for TB

The TB epidemic is strongly influenced by five risk factors: undernutrition, HIV infection, alcohol use disorders, smoking (especially among men) and diabetes (Table 9).

Update in the global tuberculosis report 2024: new definition of undernutrition

In contrast with previous years, undernutrition is defined as a BMI <18.5 kg/m² for adults and a BMI of <-2 standard deviation below the median for adolescents and children. In previous years, WHO produced estimates of attributable cases to undernourishment, defined as a BMI <16 kg/m² and the proportion of the population whose habitual food consumption is insufficient to provide the dietary energy levels that are required to maintain a normal active and healthy life.

In 2023, WHO and the University of Düsseldorf performed a systematic review and meta-analysis to determine the prognostic value of undernutrition in the general population of adults, adolescents, and children for predicting tuberculosis disease over any time. 51 cohort studies were included with over 27 million participants from the six WHO regions. These studies included sixteen large population-based studies in China, Singapore, South Korea, and the USA, and 25 studies focused on people living with HIV, which were mainly conducted in the African region. Most studies were in adults, four in children, and three in children and adults. Undernutrition as an exposure was usually defined according to standard criteria. It was shown that undernutrition may increase the risk of TB disease (RR 1.95, 95% CI 1.72 to 2.20). These results were used to estimate the attributable cases to undernutrition in 2023.

13.1 Risk ratios

Separate meta-analyses were performed to estimate the relative risks (RR) and their 95% confidence interval (95% CI), for undernutrition, alcohol use disorders, smoking and diabetes. The RR and 95%CI for HIV infection was calculated from the estimated incidence of TB in people living with HIV and HIV-negative people using the following formula.

$$RR_{HIV} = \frac{CI_{HIV+}}{CI_{HIV-}}$$

where CI_{HIV+} is the estimated incidence of TB among people living with HIV in 2023 and CI_{HIV-} is the estimated incidence of TB among HIV-negative people in 2023.

Standard deviation for RR_{HIV} was computed using the second-order Taylor expansion formula.

13.2 Exposed population

The total exposed population was calculated as the product of the total population in 2023 (for undernutrition and HIV infection) or the adult population in 2023 (for alcohol use disorders, smoking and diabetes) and the proportion of the population affected by the corresponding risk factor (P_e).

The proportion of the population affected by the different risk factors were obtained on 2 July 2024 from the following indicators in the WHO Global Health Observatory at <https://www.who.int/data/gho>:

| Risk factor | WHO Global Health Observatory indicator |
|-----------------------|---|
| Alcohol use disorders | Prevalence of underweight among adults, BMI < 18.5 (crude estimate) (%) |
| Diabetes | Raised fasting blood glucose (≥ 7.0 mmol/L or on medication)(age-standardized estimate) |
| HIV infection | Prevalence of HIV among adults aged 15 to 49 (%) |
| Smoking | Estimate of current tobacco smoking prevalence (%) (age-standardized rate) |
| Undernutrition | Prevalence of underweight among adults, BMI < 18.5 (crude estimate) (%) |

13.3 Population attributable fraction

The population attributable fraction (*PAF*) is the proportion of incident TB cases in a population that is attributable to a given risk factor, and was calculated using the following formula:

$$PAF = \frac{P_e(RR - 1)}{1 + P_e(RR - 1)}$$

13.4 Attributable TB cases

The attributable incidence rate in 2023 and its standard deviation were estimated using the second-order Taylor expansion formula as the product of the incidence rate of TB in the total population (for undernutrition and HIV infection) or the adult population (for alcohol use disorders, smoking and diabetes) and the *PAF*. The estimated number of attributable TB cases was then calculated as the product of the attributable incidence rate and the total population (for undernutrition and HIV infection) or the adult population (for alcohol use disorders, smoking and diabetes).

Table 9. Attributable risk for TB in 2023

| Risk Factor | Relative risk (uncertainty interval) | Exposed population (millions) | PAF (%) | Attributable TB cases (millions, uncertainty interval) |
|----------------------------|---|--|--------------------|---|
| Alcohol use disorders [50] | 3.3 (2.1-5.2) | 286 | 7.8 | 0.7 (0.5-1.0) |
| Diabetes[51] | 1.5 (1.3-1.8) | 502 | 4.0 | 0.4 (0.3-0.5) |
| HIV infection[52] | 13 (11-15) | 39 | 5.6 | 0.6 (0.6-0.7) |
| Smoking[53] | 1.6 (1.2-2.1) | 943 | 7.3 | 0.7 (0.5-1.0) |
| Undernutrition[54] | 2.0 (1.7-2.2) | 616 | 8.9 | 1.0 (0.8-1.1) |

14. Conclusion

The methods described here can be combined to assess tuberculosis incidence and mortality, to evaluate progress towards targets for TB control and the Sustainable Development Goals (SDGs) for TB. Alternative TB burden estimation methods have been developed by the Institute of Health Metrics and Evaluation [55], with generally consistent results at the global level compared with WHO, but with marked differences in specific countries. Discrepancies in estimates from different agencies reflect the questionable quality and completeness of the underlying data. Further convergence in estimates will result from improvements in measurements at country level. National TB programmes should be able to measure the level and time trends in incidence through well-performing TB surveillance with universal access to healthcare. In countries with incomplete routine surveillance, prevalence surveys of TB disease provide estimates of TB burden that do not heavily rely on expert opinion. The performance of TB surveillance should be assessed periodically [10] and the level of under-reporting should be measured [9] and minimized. TB mortality will ideally be measured by counting deaths in a comprehensive vital registration system.

WHO's post-2015 global TB strategy, known as the End TB Strategy [56] has the goal of ending the global TB epidemic, with corresponding targets of a 90% reduction in TB deaths and an 80% reduction in the TB incidence rate by 2030, compared with 2015. However, the milestones set for 2020 were still far from being achieved in 2023. The COVID-19 pandemic has caused enormous health, social and economic impacts since 2020. This includes impacts on the provision of and access to essential TB services, the number of people diagnosed with TB and notified as TB cases through national disease surveillance systems, and TB disease burden (incidence and mortality). Intensified efforts and increased funding are urgently needed to reverse the negative impact of the pandemic.

Acknowledgements

Ibrahim Abubakar, Sandra Alba, Elisabeth Allen, Martien Borgdorff, Jaap Broekmans, Ken Castro, Frank Cobelens, Ted Cohen, Charlotte Colvin, Sarah Cook-Scalise, Liz Corbett, Simon Cousens, Katherine Fielding, Peter Godfrey-Faussett, Yohhei Hamada, Rein Houben, Helen Jenkins, Avinash Kanchar, Li Liu, Mary Mahy, Valérie Schwoebel, Cherise Scott, James Seddon, Babis Sismanidis, Andrew Thomson, Edine Tiemersma, Theo Vos, Emilia Vynnycky and Richard White reviewed the described methods to derive TB incidence, prevalence and mortality with disaggregation by age and sex for the period of 2000-2019 and provided specific recommendations to improve them. Nicholas A. Menzies, Hsien-Ho Lin and Finn McQuaid provided critical review of the initial transmission dynamic modelling to estimate the impact of COVID-19-related disruptions on TB incidence and mortality. Members of a subgroup of the WHO Task Force on TB Impact Measurement reviewed methodological updates to the dynamic modelling as well as new methods for generating the time series of RR-TB in a meeting held in Geneva in May 2022. The subsequent in-depth review provided by Nicholas A. Menzies, Finn McQuaid, Roel Baker and Richard White provided valuable further contributions. Sandip Mandal and Kirankumar Rade for the revision and implementation of the methods used to estimate incidence and mortality in India. Finally, a special thanks to Philippe Glaziou (who led WHO's work related to TB disease burden estimation from 2008–2022) for his advice on the use, implementation and updating (as appropriate) of previous methods and codes.

Annex 1 - Definitions

Incidence is defined as the number of new and recurrent (relapse) episodes of TB (all forms) occurring in a given year. Recurrent episodes are defined as a new episode of TB in people who have had TB in the past and for whom there was bacteriological confirmation of cure and/or documentation that treatment was completed.

Prevalence is defined as the number of TB cases (all forms) at the middle of the year.

Mortality from TB is defined as the number of deaths caused by TB in HIV-negative people occurring in a given year, according to the latest revision of the International classification of diseases (ICD-10). TB deaths among people living with HIV are classified as HIV deaths in ICD-10. For this reason, estimates of deaths from TB in people living with HIV are presented separately from those in HIV-negative people.

The **case fatality rate** is the risk of death from TB among people with active TB disease.

The **case notification** rate refers to new and recurrent episodes of TB notified for a given year. Patients reported in the *unknown history* category are considered incident TB episodes (new or recurrent).

Population estimates were obtained from the World Population Prospects, which is produced by the United Nations Population Division (UNPD, <http://esa.un.org/unpd/wpp/>). The UNPD estimates sometimes differ from those made by countries.

References

1. Dye C, Bassili A, Bierrenbach AL, Broekmans JF, Chadha VK, Glaziou P, Gopi PG, Hosseini M, Kim SJ, Manissero D, Onozaki I, Rieder HL, Scheele S, van Leth F, van der Werf M, Williams BG. Measuring tuberculosis burden, trends, and the impact of control programmes [Internet]. Vol. 8, The Lancet Infectious Diseases. 2008. p. 233–43. Available from: [http://dx.doi.org/10.1016/s1473-3099\(07\)70291-8](http://dx.doi.org/10.1016/s1473-3099(07)70291-8)
2. Styblo K. The Relationship between the risk of tuberculous infection and the risk of developing infectious tuberculosis. Bulletin of the International Union against Tuberculosis and Lung Diseases. 1985;117–9.
3. van Leth F, van der Werf MJ, Borgdorff MW. Prevalence of tuberculous infection and incidence of tuberculosis: a re-assessment of the Styblo rule. Bull World Health Organ [Internet]. 2008 Jan;86(1):20–6. Available from: <https://www.ncbi.nlm.nih.gov/pubmed/18235886>
4. Dinnes J, Deeks J, Kunst H, Gibson A, Cummins E, Waugh N, Drobniewski F, Lalvani A. A systematic review of rapid diagnostic tests for the detection of tuberculosis infection. Health Technol Assess [Internet]. 2007 Jan;11(3):1–196. Available from: <http://dx.doi.org/10.3310/hta11030>
5. Eilers PHC, Borgdorff MW. Modeling and correction of digit preference in tuberculin surveys. Int J Tuberc Lung Dis [Internet]. 2004 Feb;8(2):232–9. Available from: <https://www.ncbi.nlm.nih.gov/pubmed/15139453>
6. Rieder HL. Methodological issues in the estimation of the tuberculosis problem from tuberculin surveys. Tuber Lung Dis [Internet]. 1995;76:114–21. Available from: http://ac.els-cdn.com/0962847995905529/1-s2.0-0962847995905529-main.pdf?_tid=c07e572e-6b37-11e2-a32a-00000aacb360&acdnat=1359589977_76de43cdb6962b4403e18004d77ee7f5
7. Sudre P, Dam HGT, Kochi A. Tuberculosis : a global overview of the situation today / P. Sudre, G. ten Dam & A. Kochi. Bulletin of the World Health Organization 1992 ; 70(2) : 149-159 [Internet]. 1992 [cited 2020 Jul 9]; Available from: <https://apps.who.int/iris/handle/10665/49275>
8. Dye C, Scheele S, Dolin P, Pathania V, Raviglione MC, for the WHO Global Surveillance and Monitoring Project. Global Burden of Tuberculosis [Internet]. Vol. 282, JAMA. 1999. p. 677. Available from: <http://dx.doi.org/10.1001/jama.282.7.677>
9. World Health Organization. Assessing tuberculosis under-reporting through inventory studies [Internet]. apps.who.int; 2012 [cited 2022 Oct 8]. Available from: https://apps.who.int/iris/bitstream/handle/10665/78073/9789241504942_eng.pdf

10. World Health Organization. Standards and benchmarks for tuberculosis surveillance and vital registration systems: checklist and user guide [Internet]. apps.who.int; 2014 [cited 2022 Oct 8]. Available from: https://apps.who.int/iris/bitstream/handle/10665/112673/9789241506724_eng.pdf
11. WHO Global Task Force on TB Impact Measurement: Improving estimation of TB disease burden via systematic assessment of surveillance data [Internet]. [cited 2022 Oct 11]. Available from: <https://www.who.int/groups/global-task-force-on-tb-impact-measurement/meetings/2010-11>
12. Dye C. The Population Biology of Tuberculosis [Internet]. Vol. 1. Princeton University Press; 2017. 278 p. Available from: <http://dx.doi.org/10.23943/princeton/9780691154626.001.0001>
13. Viechtbauer W. Conducting meta-analyses in R with the metafor package [Internet]. Vol. 36, Journal of Statistical Software. 2010. p. 1–48. Available from: <https://doi.org/10.18637/jss.v036.i03>
14. Bassili A, Grant AD, El-Mohgazy E, Galal A, Glaziou P, Seita A, Abubakar I, Bierrenbach AL, Crofts JP, van Hest NA. Estimating tuberculosis case detection rate in resource-limited countries: a capture-recapture study in Egypt. *Int J Tuberc Lung Dis* [Internet]. 2010 Jun;14(6):727–32. Available from: <https://www.ncbi.nlm.nih.gov/pubmed/20487611>
15. Huseynova S, Hashim DS, Tbena MR, Harris R, Bassili A, Abubakar I, Glaziou P, Floyd K, van Hest NA. Estimating tuberculosis burden and reporting in resource-limited countries: a capture-recapture study in Iraq. *Int J Tuberc Lung Dis* [Internet]. 2013 Apr;17(4):462–7. Available from: <http://dx.doi.org/10.5588/ijtld.12.0209>
16. van Hest NAH, Smit F, Baars HWM, De Vries G, De Haas PEW, Westenend PJ, Nagelkerke NJD, Richardus JH. Completeness of notification of tuberculosis in The Netherlands: how reliable is record-linkage and capture-recapture analysis? *Epidemiol Infect* [Internet]. 2007 Aug;135(6):1021–9. Available from: <http://dx.doi.org/10.1017/S0950268806007540>
17. Anderson, Moore, Kruijshaar, Pedrazzoli. Tuberculosis in the UK: Annual report on tuberculosis surveillance in the UK, 2010. London: Health Protection.
18. Bassili A, Al-Hammadi A, Al-Absi A, Glaziou P, Seita A, Abubakar I, Bierrenbach AL, van Hest NA. Estimating the tuberculosis burden in resource-limited countries: a capture-recapture study in Yemen. *Int J Tuberc Lung Dis* [Internet]. 2013 Apr;17(4):456–61. Available from: <http://dx.doi.org/10.5588/ijtld.11.0483>
19. Mathers CD, Fat DM, Inoue M, Rao C, Lopez AD. Counting the dead and what they died from: an assessment of the global status of cause of death data. *Bull World Health Organ* [Internet]. 2005 Mar;83(3):171–7. Available from: <http://dx.doi.org/S0042-96862005000300009>

20. Corbett EL, Watt CJ, Walker N, Maher D, Williams BG, Raviglione MC, Dye C. The growing burden of tuberculosis: global trends and interactions with the HIV epidemic. *Arch Intern Med* [Internet]. 2003 May 12;163(9):1009–21. Available from: <http://dx.doi.org/10.1001/archinte.163.9.1009>
21. Tiemersma EW, van der Werf MJ, Borgdorff MW, Williams BG, Nagelkerke NJD. Natural history of tuberculosis: duration and fatality of untreated pulmonary tuberculosis in HIV negative patients: a systematic review. *PLoS One* [Internet]. 2011 Apr 4;6(4):e17601. Available from: <http://dx.doi.org/10.1371/journal.pone.0017601>
22. Straetemans M, Glaziou P, Bierrenbach AL, Sismanidis C, van der Werf MJ. Assessing Tuberculosis Case Fatality Ratio: A Meta-Analysis. *PLoS One* [Internet]. 2011 Jun 27 [cited 2019 Mar 20];6(6):e20755. Available from: <https://journals.plos.org/plosone/article/file?id=10.1371/journal.pone.0020755&type=printable>
23. Mukadi YD, Maher D, Harries A. Tuberculosis case fatality rates in high HIV prevalence populations in sub-Saharan Africa. *AIDS* [Internet]. 2001 Jan 26;15(2):143–52. Available from: <http://dx.doi.org/10.1097/00002030-200101260-00002>
24. Ku HH. Notes on the use of propagation of error formulas. *J Res Natl Bur Stand* [Internet]. 1966 Oct;70C(4):263. Available from: <https://books.google.com/books?hl=en&lr=&id=8m4Ych3oWLYC&oi=fnd&pg=PA263&dq=Ku+HH.+Notes+on+the+use+of+propagation+of+error+formulas.+Journal+of+Research+of+the+National+Bureau+of+Standards,+Section+C:+Engineering+and+Instrumentation+1966%3B+70C:+26&ots=meUFbwuK5h&sig=KMKa4PbDDywZxyp1y5OzuMO4jio>
25. Global Task Force on TB Impact Measurement: meeting documents 2022 [Internet]. [cited 2022 Oct 12]. Available from: <https://www.who.int/groups/global-task-force-on-tb-impact-measurement/meetings/2022-05>
26. World Health Organization. Public Private Mix for TB Prevention and Care: A Roadmap. 2018.
27. Mandal S, Chadha VK, Laxminarayan R, Arinaminpathy N. Counting the lives saved by DOTS in India: a model-based approach. *BMC Med* [Internet]. 2017 Mar 3;15(1):47. Available from: <http://dx.doi.org/10.1186/s12916-017-0809-5>
28. Haario H, Saksman E, Tamminen J. An Adaptive Metropolis Algorithm. *Bernoulli* [Internet]. 2001 Apr;7(2):223. Available from: <https://www.jstor.org/stable/3318737?origin=crossref>
29. Cilloni L, Fu H, Vesga JF, Dowdy D, Pretorius C, Ahmedov S, Nair SA, Mosneaga A, Masini E, Sahu S, Arinaminpathy N. The potential impact of the COVID-19 pandemic on the tuberculosis epidemic a modelling analysis. *EClinicalMedicine* [Internet]. 2020 Nov [cited 2021 Jun 30];28:100603. Available from: <http://dx.doi.org/10.1016/j.eclinm.2020.100603>

30. Menzies NA, Wolf E, Connors D, Bellerose M, Sbarra AN, Cohen T, Hill AN, Yaesoubi R, Galer K, White PJ, Abubakar I, Salomon JA. Progression from latent infection to active disease in dynamic tuberculosis transmission models: a systematic review of the validity of modelling assumptions. *Lancet Infect Dis* [Internet]. 2018 Aug 1;18(8):e228–38. Available from: [https://doi.org/10.1016/S1473-3099\(18\)30134-8](https://doi.org/10.1016/S1473-3099(18)30134-8)
31. Andrews JR, Noubary F, Walensky RP, Cerda R, Losina E, Horsburgh CR. Risk of progression to active tuberculosis following reinfection with *Mycobacterium tuberculosis*. *Clin Infect Dis* [Internet]. 2012 Mar;54(6):784–91. Available from: <http://dx.doi.org/10.1093/cid/cir951>
32. Romanowski K, Balshaw RF, Benedetti A, Campbell JR, Menzies D, Ahmad Khan F, Johnston JC. Predicting tuberculosis relapse in patients treated with the standard 6-month regimen: an individual patient data meta-analysis. *Thorax* [Internet]. 2019 Mar;74(3):291–7. Available from: <http://dx.doi.org/10.1136/thoraxjnl-2017-211120>
33. Menzies D, Benedetti A, Paydar A, Martin I, Royce S, Pai M, Vernon A, Lienhardt C, Burman W. Effect of duration and intermittency of rifampin on tuberculosis treatment outcomes: a systematic review and meta-analysis. *PLoS Med* [Internet]. 2009 Sep;6(9):e1000146. Available from: <http://dx.doi.org/10.1371/journal.pmed.1000146>
34. Weis SE, Slocum PC, Blais FX, King B, Nunn M, Matney GB, Gomez E, Foresman BH. The effect of directly observed therapy on the rates of drug resistance and relapse in tuberculosis. *N Engl J Med* [Internet]. 1994 Apr 28;330(17):1179–84. Available from: <http://dx.doi.org/10.1056/NEJM199404283301702>
35. Guerra-Assunção JA, Houben RMGJ, Crampin AC, Mzembe T, Mallard K, Coll F, Khan P, Banda L, Chiwaya A, Pereira RPA, McNerney R, Harris D, Parkhill J, Clark TG, Glynn JR. Recurrence due to relapse or reinfection with *Mycobacterium tuberculosis*: a whole-genome sequencing approach in a large, population-based cohort with a high HIV infection prevalence and active follow-up. *J Infect Dis* [Internet]. 2015 Apr 1;211(7):1154–63. Available from: <http://dx.doi.org/10.1093/infdis/jiu574>
36. Johnson LF, Dorrington RE, Moolla H. Progress towards the 2020 targets for HIV diagnosis and antiretroviral treatment in South Africa. *South Afr J HIV Med* [Internet]. 2017 Jul 27;18(1):694. Available from: <http://dx.doi.org/10.4102/sajhivmed.v18i1.694>
37. Dodd PJ, Sismanidis C, Glaziou P. Methods for estimating tuberculosis incidence and mortality by age and sex. *Int J Epidemiol* [Internet]. 2021 Feb 24 [cited 2021 Feb 24]; Available from: <http://dx.doi.org/10.1093/ije/dyaa257>
38. World Health Organization. Definitions and reporting framework for tuberculosis - 2013 revision (updated December 2014 and January 2020) [Internet]. World Health Organization; 2013. Available from: https://apps.who.int/iris/bitstream/handle/10665/79199/9789246505340_ara.pdf

39. Van Hest NAH, Story A, Grant AD, Antoine D, Crofts JP, Watson JM. Record-linkage and capture–recapture analysis to estimate the incidence and completeness of reporting of tuberculosis in England 1999–2002. *Epidemiology & Infection* [Internet]. 2008 Dec;136(12):1606–16. Available from: <https://www.cambridge.org/core/journals/epidemiology-and-infection/article/recordlinkage-and-capturerecapture-analysis-to-estimate-the-incidence-and-completeness-of-reporting-of-tuberculosis-in-england-19992002/A237D547552C0223B27810ECC7D64BB3>
40. Lestari T, Probandari A, Hurtig AK, Utarini A. High caseload of childhood tuberculosis in hospitals on Java Island, Indonesia: a cross sectional study. *BMC Public Health* [Internet]. 2011;11(1):784. Available from: <http://www.biomedcentral.com/1471-2458/11/784/>
41. Coghlan R, Gardiner E, Amanullah F, Ihekweazu C, Triasih R, Grzemska M, Sismanidis C. Understanding Market Size and Reporting Gaps for Paediatric TB in Indonesia, Nigeria and Pakistan: Supporting Improved Treatment of Childhood TB in the Advent of New Medicines. *PLoS One* [Internet]. 2015 Oct 13 [cited 2018 Dec 5];10(10):e0138323. Available from: <https://journals.plos.org/plosone/article/file?id=10.1371/journal.pone.0138323&type=printable>
42. Horton KC, MacPherson P, Houben RMGJ, White RG, Corbett EL. Sex Differences in Tuberculosis Burden and Notifications in Low- and Middle-Income Countries: A Systematic Review and Meta-analysis. *PLoS Med* [Internet]. 2016 Sep;13(9):e1002119. Available from: <http://dx.doi.org/10.1371/journal.pmed.1002119>
43. Dodd PJ, Gardiner E, Coghlan R, Seddon JA. Burden of childhood tuberculosis in 22 high-burden countries: a mathematical modelling study. *Lancet Glob Health* [Internet]. 2014 Aug;2(8):e453–9. Available from: [http://dx.doi.org/10.1016/S2214-109X\(14\)70245-1](http://dx.doi.org/10.1016/S2214-109X(14)70245-1)
44. Dodd PJ, Yuen CM, Sismanidis C, Seddon JA, Jenkins HE. The global burden of tuberculosis mortality in children: a mathematical modelling study. *Lancet Glob Health* [Internet]. 2017 Sep;5(9):e898–906. Available from: [http://dx.doi.org/10.1016/S2214-109X\(17\)30289-9](http://dx.doi.org/10.1016/S2214-109X(17)30289-9)
45. World Health Organization. Guidance for the surveillance of drug resistance in tuberculosis: Sixth edition.
46. Stan Development Team. Stan Modeling Language Users Guide and Reference Manual [Internet]. 2021. Available from: <https://mc-stan.org>
47. Mortality and causes of death in South Africa, 2010: Findings from death notification [Internet]. [cited 2016 Sep]. Available from: <http://www.statssa.gov.za/publications/p03093/p030932010.pdf>
48. World Health Organization. WHO consolidated guidelines on tuberculosis. Module 1:

- prevention: tuberculosis preventive treatment [Internet]. World Health Organization; 2020. Available from: <https://apps.who.int/iris/handle/10665/331170>.
49. World Health Organization. WHO consolidated guidelines on tuberculosis: Module 2: screening – systematic screening for tuberculosis disease [Internet]. Geneva: World Health Organization; 2021. Available from: <https://www.who.int/publications/i/item/9789240022676>
 50. Imtiaz S, Shield KD, Roerecke M, Samokhvalov AV, Lönnroth K, Rehm J. Alcohol consumption as a risk factor for tuberculosis: meta-analyses and burden of disease. *Eur Respir J* [Internet]. 2017 Jul;50(1). Available from: <http://dx.doi.org/10.1183/13993003.00216-2017>
 51. Hayashi S, Chandramohan D. Risk of active tuberculosis among people with diabetes mellitus: systematic review and meta-analysis. *Trop Med Int Health* [Internet]. 2018 Oct;23(10):1058–70. Available from: <http://dx.doi.org/10.1111/tmi.13133>
 52. The Global Health Observatory [Internet]. [cited 2022 Nov 23]. Available from: <https://www.who.int/data/gho>
 53. Lönnroth K, Castro KG, Chakaya JM, Chauhan LS, Floyd K, Glaziou P, Raviglione MC. Tuberculosis control and elimination 2010–50: cure, care, and social development. *Lancet* [Internet]. 2010;375:1814–29. Available from: <http://dx.doi.org/10.1016/S0140>
 54. Franco JV, Bongaerts B, Metzendorf MI, Risso A, Guo Y, Peña Silva L, Boeckmann M, Schlesinger S, Damen JA, Richter B, Baddeley A, Bastard M, Carlqvist A, Garcia-Casal MN, Hemmingsen B, Mavhunga F, Manne-Goehler J, Viney K. Undernutrition as a risk factor for tuberculosis disease. *Cochrane Database Syst Rev*. 2024 Jun 11;6(6):CD015890. doi: 10.1002/14651858.CD015890.pub2. PMID: 38860538; PMCID: PMC11165671.
 55. Murray CJL, Ortblad KF, Guinovart C et al. Global, regional, and national incidence and mortality for HIV, tuberculosis, and malaria during 1990–2013: a systematic analysis for the Global Burden of Disease Study 2013. *Lancet* [Internet]. 2014 Sep 13;384(9947):1005–70. Available from: <https://www.sciencedirect.com/science/article/pii/S0140673614608448>
 56. Uplekar M, Weil D, Lönnroth K, Jaramillo E, Lienhardt C, Dias HM, Falzon D, Floyd K, Gargioni G, Getahun H, Others. WHO's new End TB Strategy. *Lancet* [Internet]. 2015;385(9979):1799–801. Available from: [https://www.thelancet.com/journals/lancet/article/PIIS0140-6736\(15\)60570-0/fulltext](https://www.thelancet.com/journals/lancet/article/PIIS0140-6736(15)60570-0/fulltext)